AD-A179 523

(12)

ARL-TR-87-6

SYNOPSIS OF AN INVESTIGATION OF THE ACOUSTICAL PROPERTIES OF SEA ICE
FINAL REPORT UNDER CONTRACT
N00014-84-C-0198

Paul J. Vidmar

APPLIED RESEARCH LABORATORIES
THE UNIVERSITY OF TEXAS AT AUSTIN
POST OFFICE BOX 8029, AUSTIN, TEXAS 78713-8029

3 February 1987

Final Report

1 February 1984 – 30 September 1985

Prepared for

OFFICE OF NAVAL RESEARCH
DEPARTMENT OF THE NAVY
WASHINGTON, DC 22217

DTIC
ELECTE
APR 23 1987
E

REPORT DOCUMENTATION PAGE		Form Approved OMB No 0704-0188

1a REPORT SECURITY CLASSIFICATION UNCLASSIFIED	1b RESTRICTIVE MARKINGS
2a SECURITY CLASSIFICATION AUTHORITY	3 DISTRIBUTION / AVAILABILITY OF REPORT Approved for public release; distribution unlimited.
2b DECLASSIFICATION DOWNGRADING SCHEDULE	
4 PERFORMING ORGANIZATION REPORT NUMBER(S) ARL-TR-87-6	5 MONITORING ORGANIZATION REPORT NUMBER(S)

6a NAME OF PERFORMING ORGANIZATION Applied Research Laboratories	6b OFFICE SYMBOL (If applicable)	7a NAME OF MONITORING ORGANIZATION Office of Naval Research
6c ADDRESS (City, State, and ZIP Code) The University of Texas at Austin Austin, Texas 78713-8029		7b ADDRESS (City, State, and ZIP Code) Department of the Navy Arlington, Virginia 22217
8a NAME OF FUNDING SPONSORING ORGANIZATION	8b OFFICE SYMBOL (If applicable)	9 PROCUREMENT INSTRUMENT IDENTIFICATION NUMBER N00014-84-C-0195

8c ADDRESS (City, State and ZIP Code)	10 SOURCE OF FUNDING NUMBERS			
	PROGRAM ELEMENT NO 62759	PROJECT NO	TASK NO	WORK UNIT ACCESSION NO

11 TITLE (Include Security Classification)

Synopsis of an Investigation of the Acoustical Properties of Sea Ice

12 PERSONAL AUTHOR(S)
Vidmar, Paul J.

13a TYPE OF REPORT final report	13b TIME COVERED FROM 84-2-1 TO 85-9-30	14 DATE OF REPORT (Year, Month, Day) 87-2-3	15 PAGE COUNT 79

16 SUPPLEMENTARY NOTATION

COSATI CODES			18 SUBJECT TERMS (Continue on reverse if necessary and identify by block number)
FIELD	GROUP	SUB GROUP	compressional velocity sea ice cores 5-50 kHz; depth dependence penetrator anisotropy temperature dependence ultrasonic Arctic ice

19 ABSTRACT (Continue on reverse if necessary and identify by block number)

This report summarizes research carried out at Applied Research Laboratories, The University of Texas at Austin (ARL:UT), under Contract N00014-84-C-0195, 1 February 1984 - 30 September 1985. The goal of this research was to determine the fundamental acoustical properties of sea ice. Our major accomplishment was measuring the temperature dependence, depth dependence, and anisotropy of the propagation velocity of ultrasonic compressional wave pulses in sea ice cores. Additional work was done to examine methods for in situ measurement of compressional and shear wave velocity and attenuation of Arctic ice.

20 DISTRIBUTION AVAILABILITY OF ABSTRACT ☐ UNCLASSIFIED/UNLIMITED ☒ SAME AS RPT ☐ DTIC USERS	21 ABSTRACT SECURITY CLASSIFICATION UNCLASSIFIED	
22a NAME OF RESPONSIBLE INDIVIDUAL Clark S. Penrod	22b TELEPHONE (Include Area Code) 512-835-3478	22c OFFICE SYMBOL

DD Form 1473, JUN 86   Previous editions are obsolete   SECURITY CLASSIFICATION OF THIS PAGE

TABLE OF CONTENTS

Accession For

NTIS GRA&I

DTIC TAB

Unannounced ☐

Justification

By

Distribution/

Availability Codes

Dist	Avail and/or Special
A-1	

QUALITY INSPECTED 1

LIST OF FIGURES

I. INTRODUCTION

Extensive studies of the mechanical properties and structure of sea ice (reviewed in Refs. 1 and 2) have found sea ice to be a complicated material and suggest that sea ice has correspondingly complicated acoustical properties. Sea ice has a brine filled pore structure with air inclusions. Thus, sea ice is a multi-component medium whose propagation velocity and attenuation will depend on frequency.[3,4] Temperature, density, salinity, porosity, and pressure depend on depth into the ice sheet, suggesting that velocities of sea ice may also depend on depth. The observed tendency of the pore structure to be vertically aligned raises the possibility that sea ice is an anisotropic medium, with vertical velocities larger than horizontal velocities.[5] The observed alignment of the optical axis (c-axis) of ice crystals in the horizontal plane indicates that acoustic velocities may also depend on direction in the horizontal plane. It is possible, then, that sea ice is a complicated, depth dependent, anisotropic medium whose velocities and attenuations change with frequency.

This report summarizes research carried out at Applied Research Laboratories, The University of Texas at Austin (ARL:UT), under Contract N00014-84-C-0195, 1 February 1984 - 30 September 1985. The goal of this research was to determine the fundamental acoustical properties of sea ice. Our major accomplishment was measuring the temperature dependence, depth dependence, and anisotropy of the propagation velocity of ultrasonic compressional wave pulses in sea ice cores. These measurements are described in Ref. 6, which is also contained in Appendix A. Additional work was done to examine methods for in situ measurement of the frequency dependence of compressional and shear wave velocity and attenuation of Arctic ice. Appendix B lists documentation produced under this contract.

Our measurement of the acoustical properties of Arctic ice was carried out on ice cores from the Bering Sea that were recovered by the U.S. Army Corps of Engineers Cold Regions Research and Engineering Laboratory (CRREL) and stored at their facilities in Hanover, New Hampshire. Since the strength tests of the ice cores would destroy their structure, we concentrated on rapidly carrying out our measurements while the cores were still intact. Rather than developing new instrumentation, we modified existing equipment that had been used to measure shear and compressional velocites

velocities at 45° to the c-axis which were both faster and slower than velocities parallel to the c-axis. We conclude that the vertically oriented pore structure of sea ice, as well as the alignment of the c-axes of the ice crystals, has an important role in determining velocity anisotropy in sea ice.

Research on methods for in situ measurement of the frequency dependence of compressional and shear wave velocity and attenuation of Arctic ice was carried out by Dr. Ching H. Yew, Department of Aerospace Engineering and Engineering Mechanics, The University of Texas at Austin. Dr. Yew renewed his interest in understanding acoustic propagation in ice and examined the use of penetrators[10] to measure the properties of Arctic ice. He also carried out a preliminary test of a broadband technique for in situ measurement of the frequency dependence of shear and compressional velocities and attenuations. His interest in the properties of Arctic ice has continued beyond the end of this contract. He is currently supervising a doctoral student who is developing a porous media theory of propagation in sea ice.[5]

The remainder of this report is organized as follows. Section II summarizes our measurement of the acoustical properties of sea ice. Section III reviews work done to examine new methods for the in situ measurement of compressional and shear wave properties of sea ice.

II. COMPRESSIONAL VELOCITY OF SEA ICE CORES

This section contains a brief review of our measurements of the propagation velocity of ultrasonic compressional wave pulses in sea ice cores. A detailed description is given in Ref. 6 and is also contained in Appendix A. Our data were obtained from five sea ice cores stored at CRREL in Hanover, New Hampshire. Measurements were made with an ultrasonic profilometer originally designed to measure compressional velocity of marine sediment cores.[11,12] Data were taken on the propagation in vertical and horizontal directions at three temperatures and several depths into the ice sheet. Horizontal velocities were measured at three orientations with respect to the c-axis. We did not examine the effects of density, salinity, porosity, ice structure, temperature gradients, or pressure.

A.   Background

Past measurements of the compressional velocity of sea ice provided typical values for the velocity and its dependence on salinity, temperature, and depth. Ultrasonic measurements made on samples from Arctic sea ice gave typical values of compressional velocity between 2100 and 3800 m/s.[13,14] Compressional velocity decreases with increasing salinity and increases with decreasing temperature.[14] Other ultrasonic measurements showed that compressional velocity depends on depth in ice crystallized from salt water.[15] Seismic studies[16] of sea ice have also been carried out and provided values for the average velocity for the ice layer that agree with ultrasonic measurements.

Acoustic anisotropy in ice is expected from the directional characteristics of ice crystals and has been observed in laboratory studies of fresh water ice and ultrasonic measurements on fresh water ice cores. Laboratory studies[7] found that the compressional velocity parallel to the c-axis exceeds that perpendicular to the c-axis by about 15% at atmospheric pressure, and that the two velocities become equal at a pressure of about 500 atm. Ultrasonic measurements made on samples of ice from the thick fresh water ice sheets (in which the c-axis tends to be vertically oriented) in Antarctica and Greenland[8,9] also show that the compressional velocity parallel to the c-axis (vertical) is slightly higher (1-2%) than that perpendicular to the c-axis

of anisotropy are comparable, our data showed that the anisotropy in sea ice is qualitatively different from that found in fresh water ice. In our data from sea ice cores, the vertical velocity (perpendicular to the sea axis) was consistently faster than the horizontal velocity parallel to the c-axis. In fresh water ice, the velocity parallel to the c-axis is faster than the perpendicular velocity.[10-12] Our data agrees with recent theoretical work[5] showing that the vertically oriented pore structure of sea ice can cause the vertical velocity to exceed the horizontal velocity by as much as a factor of 2. Apparently the large scale vertically oriented pore structure of sea ice, as well as the alignment of the ice crystals, has an important role in determining the acoustic anisotropy of sea ice. In agreement with data from fresh water ice, we found that velocities parallel to the c-axis are faster than horizontal velocities perpendicular to the c-axis. Horizontal velocities at 45° to the c-axis were found to be either faster or slower than velocities parallel to the c-axis, depending primarily on temperature.

Additional factors (temperature gradients, pressure, salinity, etc.) that we did not examine in this experiment need to be taken into account in determining the in situ properties of sea ice. Drainage of brine while coring, and some melting during our experiment, may have altered the structure of the ice cores from that found in situ. These factors should not affect our qualitative results--that sea ice has a consistent temperature dependence and is anisotropic. However, it is possible that the magnitude of these phenomena may be different in situ than in our sea ice cores.

III. METHODS FOR IN SITU MEASUREMENTS

This section describes the preliminary work done to develop a method to measure the in situ acoustical properties of Arctic ice. The concept[10] uses penetrators to deploy a group of transducers (shown schematically in Fig.1) to generate and record compressional, shear, surface, and plate waves. The acoustical sources to generate these waves are located in a near-surface penetrator. Sensors for each wave are deployed in pairs. The distance between the acoustic source and the receiver is chosen to be consistent with the frequency range of the source and attenuation of the waves being generated.

Figure 2 schematically depicts the wave generating penetrator. The source for compressional waves, surface waves, and plate waves is an electrical spark (center frequency near 80 kHz) or an exploding air bubble (center frequency near 1 kHz). The spark or bubble is located near the lower end of the penetrator. Shear waves are generated by an electrically actuated striker that would move the ice horizontally.

The dispersion and attenuation characteristics of the ice are obtained using a technique[17-20] that uses Fourier transform of the time series at two receivers at different locations. The distance between the sensors and the amplitude ratio of the transforms are used to determine the attenuation as a function of frequency. The dependence of velocity on frequency is contained in the measured phase difference of the two transforms. An inverse theory[21] can be used to determine the dependence of acoustical properties on position by comparing the measured dispersion and attenuation with theoretical predictions.

Preliminary tests of this approach were carried out using fresh water ice. The signal source was an electrical spark in air, above the ice. The acoustic signal from the spark traveled through a known thickness of ice and was detected with a piezoelectric compressional wave transducer. The measured signal was recorded digitally with a transient recorder and analyzed using a fast Fourier transform algorithm. Data were taken for two ice blocks with different thicknesses (instead of at two locations in the same ice block) and analyzed to obtain the attenuation and dispersion of compressional waves from 1 to 50 kHz. The success of this preliminary test was
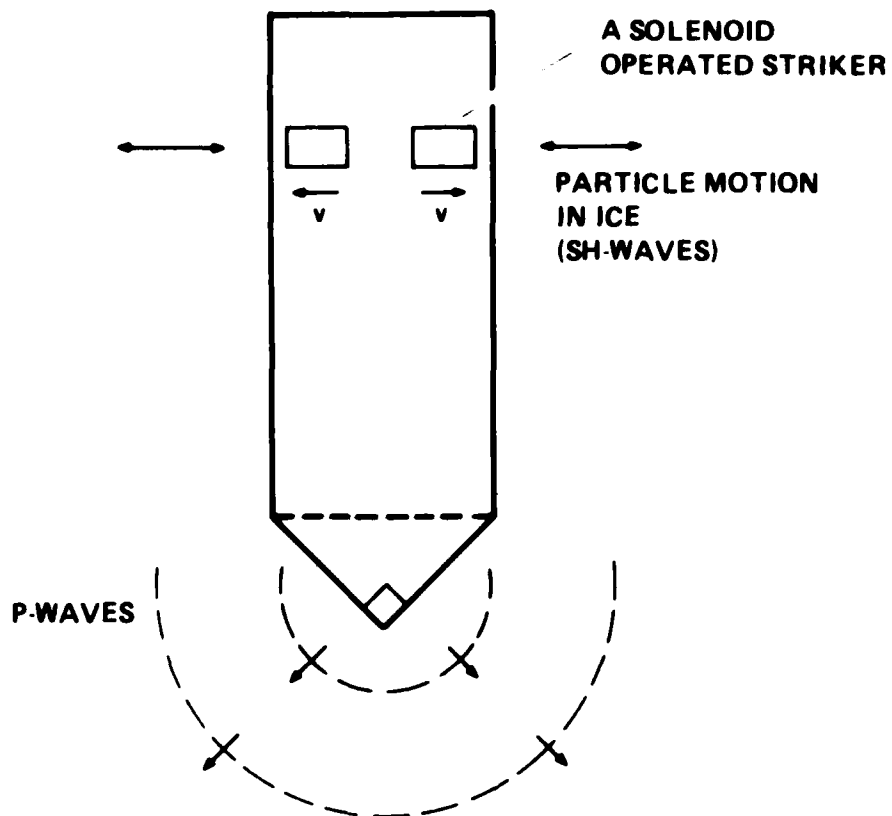
9

FIGURE 2
ACOUSTIC SOURCE PENETRATOR

11

encouraging. We believe that our approach could be further developed for making in situ measurements of sea ice characteristics.

IV. SUMMARY

From 1 February 1984 to 30 September 1985, ARL:UT carried out research under Contract N00014-84-C-0195 to determine the fundamental acoustical properties of sea ice. Our major accomplishment was measuring the temperature dependence, depth dependence, and anisotropy of the compressional velocity in sea ice cores. These measurements show that velocity increases with decreasing temperature and that gradients of compressional velocity are both positive and negative with magnitudes between 20 and 400^{-1}. Compressional velocities were found to be anisotropic with vertical velocities exceeding horizontal velocities by up to 5%, suggesting that the vertical pore structure of sea ice, as well as ice crystal structure, has an important influence on anisotropy. Additional work showed that spark sources combined with Fourier transform analysis can be used to measure the in situ velocity and attenuation of ice in the 1-50 kHz frequency range.

ACKNOWLEDGMENTS

APPENDIX A

COMPRESSIONAL WAVE VELOCITY OF SEA ICE

by

P. J. Vidmar and J. B. Lindberg

Compressional velocity of sea ice cores

Paul J. Vidmar and Jo B. Lindberg[t]
Applied Research Laboratories. The University of Texas at Austin
Austin. Texas 78713-8029

Laboratory measurements of the propagation velocity of ultrasonic compressional wave pulses were made at four orientations (vertical and at three horizontal directions) on five cores from first year sea ice. Our technique measures velocities with an accuracy of ±10% and relative velocities to within ±0 9%. Data were collected at three temperatures (-10°C, -20°C, and -23°C) and at several positions along the cores. Measured velocities were in the range of 3800-4500 m/s. Relative velocities were used to investigate the temperature dependence, depth dependence, and anisotropy of the compressional velocity. The velocity of all five cores in all four propagation directions was up to 12% higher at -20°C than at -10°C. Although the depth dependence was not consistently linear with depth, we made estimates of the average compressional velocity gradient for each core. Estimated gradients were both positive and negative and had magnitudes between 20 and 400 s^{-1}. Velocities were slightly anisotropic (generally <5%) with vertical velocity faster than horizontal velocity, horizontal velocity perpendicular to the c-axis of the ice crystals slower than velocity parallel to the c-axis, and horizontal velocity at 45° to the c-axis either faster or slower than velocity parallel to the c-axis, depending primarily on temperature [This work was supported by the Office of Naval Research.]

I. INTRODUCTION

Extensive studies of the mechanical properties and structure of sea ice[1,2] have found sea ice to be a complicated material and suggest that sea ice has correspondingly complicated acoustical properties. Sea ice, which has a brine filled pore structure with air inclusions, is a multi-component medium whose propagation velocity and attenuation could depend on frequency.[3,4] Temperature, density, salinity, porosity, and pressure depend on depth into the ice sheet, suggesting that velocities of sea ice may also depend on depth. The pore structure tends to be vertically aligned, raising the possibility that sea ice is an anisotropic medium, with horizontal velocities differing from vertical velocities.[5] The alignment of the optical axis (c-axis) of ice crystals in the horizontal plane indicates that acoustic velocities may also depend on direction in the horizontal plane. It is possible then, that sea ice is a depth dependent anisotropic medium whose velocities and attenuations change with frequency.

Past measurements of the shear and compressional velocities of sea ice provide both the typical values for velocities, and their dependence on salinity, temperature, and depth. Ultrasonic measurements made on samples from Arctic sea ice give typical compressional velocity values of between 2100 and 3800 m/s and shear velocities between 1100 and 1900 m/s.[6,7] Compressional velocity decreases with increasing salinity and increases with decreasing temperature while shear velocity is not much influenced by variations in either temperature or salinity.[7] Other ultrasonic measurements in ice crystallized from salt water[8] show that compressional velocity depends on depth. Seismic studies[9] of sea ice have also been carried out; these have provided values for the average velocity for the ice layer that agree with ultrasonic measurements on ice cores

Ice is expected to be acoustically anisotropic because of the directional characteristics of ice crystals. Anisotrophy has been observed in laboratory studies of

20

fresh water ice and ultrasonic measurements on fresh water ice cores. Laboratory studies[10] of the effects of pressure on compressional velocities found that velocities parallel to the c-axis exceed those perpendicular to the c-axis by about 15% at atmospheric pressure, but that the velocities are comparable at a pressure of 500 atm. Ultrasonic measurements made on samples of ice from the thick fresh water ice sheets (in which the c-axis tends to be vertically oriented) in Antarctica and Greenland[11,12] also show that the compressional velocity parallel to the c-axis (vertical) is slightly higher (1-2%) than that perpendicular to the c-axis (horizontal).

This paper reports laboratory measurements of the propagation velocity of ultrasonic compressional wave pulses in sea ice cores stored at the U.S. Army Corps of Engineers Cold Regions Research and Engineering Laboratory (CRREL) in Hanover, New Hampshire. Measurements were made with an ultrasonic profilometer originally designed to measure compressional velocity of marine sediment cores.[13,14] Data were taken on the propagation in vertical and horizontal directions at three temperatures and several depths into the ice sheet. Horizontal velocities were measured at three orientations with respect to the c-axis. Our technique measures velocities with an accuracy of ±10% and relative velocities to within ±0.9%. We did not examine the effects of density, salinity, porosity, ice structure, temperature gradients, or pressure.

Our data show that the compressional velocity of sea ice is anisotropic, has a fairly consistent dependence on temperature, and has a highly variable dependence on depth. Measured velocities were in the range of 3800-4500 m/s, slightly higher than those measured in earlier work.[6,7] In agreement with previous work,[7] we found that the velocity at -20° was up to 12% higher than the velocity at -10°C. This temperature dependent increase occurred for all five cores, all three propagation directions, and at all depths where data were taken. The depth dependence was not consistent from core to core. The variability of the epth dependence of velocity

21

suggested that the structure of the sea ice cores is highly variable. Although the depth dependence was not consistently linear with depth, we estimated gradients of compressional velocity. These gradients were both positive and negative and had magnitudes between 20 and 400 s^{-1}.

Our most interesting results came from observations of anisotropy. All five cores were anisotropic, with velocity differences generally about ±3%, but with maximum values of about ±5%. These velocity differences are less than the 15% measured on laboratory prepared fresh water ice[10] but larger than the 1-2% found in ice cores from the thick fresh water ice sheets in Antarctica and Greenland.[11,12] While the magnitudes of anisotropy are comparable, our data showed that the anisotropy in sea ice is qualitatively different than that found in fresh water ice. In our data from sea ice cores, the vertical velocity (perpendicular to the sea axis) was consistently faster than the horizontal velocity parallel to the c-axis. In fresh water ice, the velocity parallel to the c-axis is faster than the perpendicular velocity.[10-12] *Our data agrees with recent theoretical work*[5] showing that the vertically oriented pore structure of sea ice can cause the vertical velocity to exceed the horizontal velocity by as much as a factor of 2. The most interesting feature of our data was the observation that the measured vertical velocity is faster than velocity parallel to the c-axis (which was horizontal in the sea ice cores). Apparently, the large scale vertically oriented pore structure of sea ice, as well as the alignment of the ice crystals, has an important role in determining the acoustic anisotropy of sea ice. In agreement with data from fresh water ice, we found that velocities parallel to the c-axis are faster than horizontal velocities perpendicular to the c-axis. Horizontal velocities at 45° to the c-axis were found to be either faster or slower than velocities parallel to the c-axis, depending primarily on temperature.

Additional factors (temperature gradients, pressure, salinity, etc.) should be taken into account in determining the in situ properties of sea ice. In addition to these factors, the structure of the cores may have been altered from that in situ owing to the drainage

22

of brine while coring and some melting during our experiment. However, these factors should not affect applying our qualitative results--that sea ice has a consistent temperature dependence and is anisotropic--to in situ sea ice. It is possible that the magnitudes of these phenomena may be different in situ than in sea ice cores, though.

The remainder of this paper is organized as follows. Section II describes the profilometer, calibration, and measurement procedures. Section III gives the results of our measurements. Section IV summarizes and discusses our results.

II. INSTRUMENTATION AND PROCEDURES

To measure the compressional velocity of Arctic ice cores, we modified the ARL:UT profilometer that had previously been used to measure the compressional and shear velocities of marine sediments.[13,14] The profilometer measures the time interval between a trigger pulse applied to the transmitting transducer and its arrival at the receiving transducer. Calibration of the system removes the instrumental time delay due to phase shifts in the cables, electronic instruments, and transducers. Dividing the thickness of the sample by the transit time across the sample yields the velocity (group velocity not phase velocity). Analysis of the accuracy of our instrumentation shows that velocity can be determined to within 10%, but that relative velocities can be determined to about 1%. The profilometer, calibration, and procedure for taking data are discussed in more detail below.

A. Profilometer

The profilometer electronics had to be only slightly modified for use with ice samples stored at CRREL. The profilometer was originally designed[13,14] to measure transit times of about 30 μs, corresponding to a compressional wave with a velocity of about 1600 m/s traveling across a sediment core about 5 cm in diameter. Previous measurements[6,7] of the compressional velocity of sea ice gave values of 2100-3800 m/s. These higher velocities combined with the larger diameter of ice cores (about 10 cm in diameter) also resulted in estimates of transit time across the

23

ice cores of about 30 μs. Since the time intervals to be measured were expected to be about the same for both the marine sediment cores and the ice cores, no changes in the profilometer electronics were needed.

The profilometer measures the time interval beginning with a 1.5 μs pulse applied to the transmitting transducer and ending with the arrival of the signal at the receiving transducer. This time is given by

$$T = T_s + T_i \ ,$$

where T is the measured time interval, T_s is the transit time of the signal across the sample, and T_i is the time interval related to the measurement system electronics.

The time interval is measured as follows. The pulse to the transmitter initiates a signal (ramp) whose voltage increases linearly with time. When the pulse arrives at the receiving transducer, a trigger pulse is generated to stop the ramp. The final ramp voltage is sampled and applied to a voltage controlled oscillator. The frequency of the oscillator f is linearly proportional to the applied voltage and is accurately measured with a frequency counter. The time interval and frequency are related by

$$T = \alpha f + \beta \quad ,$$

where α is the proportionality constant between time and frequency and $-\beta/\alpha$ is the frequency when T=0. Both α and β can be adjusted in the profilometer electronics.

The arrival of the pulse at the receiving transducer is determined as follows. The received pulse is bandpass filtered between 120 and 250 kHz. The trigger pulse to stop the ramp is generated when the first peak of the received signal exceeds a threshold level. The threshold is needed to avoid triggering on low level noise from the pulse generating circuitry. An oscilloscope is used to monitor the received signal and the termination of the ramp, to adjust the amplitude of the initial pulse and an

24

attenuator in the receiver so that the trigger pulse occurs between the first and second complete oscillation of the received signal. We recorded the location of the trigger point in the received signal for each sample and took into account changes in trigger point from sample to sample in determining the travel time through the sample.

We found that the profilometer produces inaccurate measurements if the repetition rate (750 /s) of the initial pulse is too fast for the signal from one pulse to decay before the next pulse is transmitted. The received signal, in this case, is a superposition of the first arrival and other arrivals that have traveled several times through the sample, traveled along the surface of the sample, or traveled partially as shear waves. Under these conditions the ramp will not necessarily be ended by the first arrival. This was not a concern for our measurements on ice cores, since the signal on the oscilloscope verified that the absorption was high enough to completely attenuate the acoustic signal in the 1.3 ms between pulses.

In our measurements we used immersion type compressional wave transducers (Panametrics Corporation, V301) with flat faced, non-focused 1 in. diam PZT elements. The transducers are watertight so that there is no moisture trapped to freeze at low temperature and damage the PZT element. The transducers were coaxially mounted facing each other in a brass holder, which allowed their separation to be adjusted. The transducers were placed across the diameter of an ice core, moved into contact with the sample, and clamped in place. A layer of silicone based grease was used to couple the transducers to ice cores.

B.   Calibration

Calibration for measuring the compressional velocity in ice cores required a different procedure than that developed for use with marine sediment cores. Calibration for marine sediment cores uses core liners filled with liquids whose speed of sound is known. The compressional velocity of marine sediments is close to the sound of speed in water, and liquids such as fresh water, glycerine-water solutions,

and saline solutions are available for calibration. The sound speed of these liquids can be obtained from their composition and temperature. The liquid filled core liners are substituted for the sediment filled cores and the frequency of the voltage controlled oscillator measured as a function of sample velocity. Since the frequency is proportional to transit time, and transit time is proportional to the inverse of the velocity (for samples with the same size), this procedure directly defines the linear relationship between frequency and the inverse of the velocity. The calibration takes into account the instrumental time delay through the offset frequency and the dependence on length through the proportionality constant. The effects of liner material, phase shifts in the circuitry, and the sample size are automatically included in the calibration. We note that this procedure does not work if the liner material is changed (or absent), or if the sample diameter is not the same as that used in the calibration. In that case, the change in path length results in a different proportionality between the inverse of the velocity and transit time, and hence frequency.

This procedure had several problems that made it unsuitable for calibrating the profilometer to measure the compressional velocity of sea ice cores. First, the diameter of the ice cores varied from core to core and needed to be taken into account for accurate measurements of velocity. Second, using the reference liquids and doubling the sample size to that of the ice cores would result in transit times of about 60 µs, twice the transit time expected for the compressional wave in ice. Hence, the calibration could not be done in the transit time range of the data, but would have to be extrapolated. Third, we did not feel confident in being able to accurately predict the change in size and velocity of the frozen liquids needed to carry out calibration at the low temperatures at which data were collected.

Our calibration used thin rods of brass, aluminum, and polystyrene instead of liquid filled core liners. The compressional velocities (see Table I) of these materials are in the 3000-4000 m/s range expected for sea ice and they can be used at low

temperatures. Since signals travel through thin rods at a velocity which depends on the bulk parameters of the material and the diameter of the rod, it is possible to generate a wide variety of travel times for use in determining α and β, the profilometer parameters, and T_i, the instrumental component of the time delay. The small absorption of signals in the metal rods resulted in interfering arrivals due to multiple reflections that interfered, as described above, with the operation of the profilometer. During calibration, the repetition rate of the ultrasonic pulse was decreased until these interfering signals did not interfere with the initial part of the signal.

Our calibration procedure had two parts. First, we accurately determined the relationship between the frequency of the voltage controlled oscillator and the time interval measured by the profilometer. This was done by using metal rods of different lengths to generate transit times in the range that we expected to occur in our measurements on sea ice cores. The frequency of the voltage controlled oscillator was recorded and the time interval measured with an oscilloscope having a digital time delay display. A regression analysis of the dependence of frequency on travel time measured for five rods of each material found the average values and uncertainties in α and β to be: $\alpha = -2.1291 \times 10^{-8} \pm 0.0143 \times 10^{-8}$ s/Hz and $\beta = 1.5397 \times 10^{-4} \pm 0.0080 \times 10^{-4}$ s.

The second part of the calibration was to determine the instrumental component of the measured time interval. This was done by measuring T as a function of the length of several metal rods made of the same material and having the same diameter. Since the propagation velocity occurs at the rod velocity and is independent of the length of the rod, the linear relationship between time and length can be established. The instrumental component is the time when the length of the rod is set to zero. Since there is the possibility that acoustic impedance could influence T_i, measurements were carried out for three materials. These data yielded an average value for T_i of 10.60 μs and a spread of 1.43 μs.

27

We also investigated the temperature dependence of the profilometer calibration by measuring the time interval for the aluminum rods at 20°C and -20°C. Using tabulated values[15] for the coefficient of linear expansion and the temperature dependence of the adiabatic Young's modulus, we calculated that the travel time through the aluminum rods would change by about 0.02 µs between 20°C and -20°C. Since this time interval is small compared to the 0.2 µs resolution of the profilometer, any change in the time interval measured by the profilometer would indicate a temperature dependence calibration. Since no change was measured, we concluded that the calibration of the profilometer did not change significantly over this temperature range.

C. Accuracy of measurements

To estimate the accuracy of our measurements, we carried out a numerical sensitivity analysis of the equations for determining the velocity and the relative velocity from the measured sample thickness and the frequency of the voltage controlled oscillator. The velocity v is given by

$$v = L / (\alpha f + \beta - T_i) \quad ,$$

where L is the sample length, f is the frequency of the oscillator, α and β are the constants relating frequency to time and T_i is the instrumental component of the measured time interval. The relative velocity u is given by

$$u = v / v_{ref}$$

where v_{ref} is a measured velocity that is chosen as a reference.

The results of the error analysis are given in Table II. The overall error in v is about 10% (350 m/s for sea ice), caused primarily by the uncertainties in α, β, and T_i. The uncertainty in u is much smaller, less than 1%, since the uncertainties in α, β, and

28

T_i do not depend on the particular sample and will cancel to lowest order. The errors in L and f do depend on the particular measurement and the effect of their uncertainty is doubled since they could combine their effects rather than cancel. Clearly, our instrumentation is best suited for making relative velocity measurements.

D. Procedure

For each measurement, the diameter of the cylindrical ice core was placed between the transducer elements and silicone grease applied to couple the transducers to the core. After the transducers were pressed against the core and locked in place, the distance between the faces of the transducers was measured with a vernier caliper and recorded. The frequency of the oscillator measuring the travel time was then recorded. The received signal was viewed on a monitor oscilloscope and the point in the received signal where the voltage ramp terminated was recorded. The orientation of the core relative to the c-axis and the depth of the core into the ice sheet were also recorded. On the horizontal cores, measurements of the vertical and horizontal velocity across the diameter of the cylindrical core were made. On the vertical ice cores, measurements were taken at $0°$, $45°$, and $90°$ with respect to the c-axis. A total of 117 velocities were measured; 27 were vertically oriented and 30 were horizontal velocities at each orientation relative to the c-axis. Temperature was changed in the evening so that the cold room, the ice cores, and the equipment could stabilize overnight. The profilometer worked well at low temperature, and was kept inside the cold room for the duration of our experiment.

III. RESULTS

In this section, we present the results of our measurements of the compressional velocity of five sea ice cores obtained by CRREL from first-year ice in the Bering sea. The characteristics of the five sea ice cores used for our measurements are listed in Table III The cores are about 10 cm in diameter. They were cut either horizontally or vertically from the ice sheet. The horizontal cores were about 25-30 cm in length while

29

the vertical cores were about 1 m in length. Horizontal cores were cut from a large diameter vertical core. The direction of the c-axis for each core was provided by CRREL. "Air-brine" inclusions in the ice crystals were clearly visible in the cores and tended to be elongated in the c-axis direction. We also observed larger air-brine pockets in the cores, particularly in core 325, between depths of 108 cm and 125 cm. Density and salinity were not available.

The cores were stored at CRREL at -30°C to keep the brine frozen and to reduce changes in ice structure that would result with melting at higher temperatures. Our measurements were conducted in temperature controlled rooms, called cold rooms. Data were taken for both horizontal and vertical propagation at depths of 1-2 m into the ice. Measurements were made at three temperatures: first -20°, followed by -10°, and -23°. At -10° the cores were "wet" and small amounts of brine (about 5 cc) dripped from the cores. At -23° and -20° the cores were dry and no brine was lost.

Estimates of the effects of the loss of brine at -10°C on the compressional velocity showed that the change in velocity directly attributable to changes in density and salinity would not be measurable with our system. The estimates were carried out assuming that the volume of brine lost from a core was a good estimate of the change in the core's volume. The fractional changes in salinity and density were then assumed to be proportional to the fractional changes in volume. The fractional changes in volume was about 0.2% for the smaller cores. Interpreted as a change in density, this would produce an increase in velocity of about 0.1%. The effects of a change in salinity were estimated from the reported dependence of velocity on salinity[7] and an assumed salinity of 8 parts per thousand. The decrease in salinity would increase velocity by about 1.5 m/s, an increase of 0.04%. Both of these changes in velocity are far too small for us to measure.

While the loss of brine during our measurements did not have a direct influence on our measurements, the change in core structure accompanying the loss of brine

may have affected our measurements. As noted above, some of the ice began to liquify when the temperature was lowered to -10°C and a small amount of brine (about 5 cc) was observed to drip from the cores. The small changes in ice structure might have resulted in slightly different ice properties at -10°C that were retained when the temperature was decreased for our final measurements at -23°C. It is possible that the overall structure of the ice at -20°C could be different from the structure at -23°C. Only one core had a depth dependence that clearly supported this hypothesis. The relative velocities in all three horizontal directions for core 350 had a different depth dependence was at -20°C than at -10°C and -23°C. For the other four cores, the depth dependence was different at each temperature. For these cores it is possible that local changes in structure occurred, but there was not an overall change.

While we expected propagation velocities between 3000 and 3800 m/s at -10°C,[7] we found that our sound pulses traveled through the sea ice cores at slightly higher velocities. The velocities we measured (listed in the Appendix) are between 3882 and 4479 m/s. Table IV shows that the average of the velocities over depth ranges from a low of 3950 m/s to a high of 4438 m/s. The small spread about the average indicates the ability of our procedure to make accurate relative velocity measurements.

Table IV also reveals the three major features we found in our measurements of velocities of sea ice cores. First, there is a consistent dependence of velocity on temperature. The average velocities increase by about 300 m/s (about 8%) as the temperature decreases from -10°C to -20°C, and then decreases by about 100 m/s as the temperature is further decreased to -23°C. Second, there is a small anisotropy with vertical velocities as much as 220 m/s (about 5%) larger than horizontal velocities. Third, the small spread about the average velocities (< 2%) indicates that there is not a strong dependence on depth over the 75 cm depth interval of the ice cores. Each of these features will be examined in more detail below. Since the changes in velocity

31

are small, our remaining discussion will center on relative velocities which we can measure to within 1%.

A. Temperature dependence

We found that the compressional velocity increased with decreasing temperature Data taken at -20° had a consistently higher velocity, by as much as 12%, than data taken at -10°C. The increase in velocity is consistent with previous work[7] that reported the velocity at -11°C to -13°C to be 12% higher than the velocity at -5°C to -8°C. Our data at -23°C have a slightly lower velocity than those at -20°. This decrease was not expected and may not be an intrinsic feature of sea ice but, rather, may be caused by a change of ice structure accompanying the loss of some brine during data collection at -10°C.

Figure 1 illustrates some of the dependences on temperature we found in our data. Each curve in Fig. 1 was obtained by using the velocity at each depth measured at -10°C as the reference velocity in calculating the relative velocities Changing the reference velocity with depth should reduce the effects of an overall depth dependence and enhance effects due to temperature alone. The error bars indicate the expected uncertainty in the relative velocity (±0.009). We note, as mentioned above, that the loss of brine from the cores could have changed the ice structure as data were taken Figure 1(a) shows a consistent dependence on temperature at each of the three depths where measurements of vertical velocity were made on core 276 The spread about the average at -23 C and -20 C is about 0 007, within the accuracy of our measurement. Figure 1(b) has a consistent dependence at -20° (spread of 0 002) but a large spread of 0 019 at -23° The spread at -23 C indicates a depth dependence that is different than that at -20 and -10° Figure 1(c) is similar to Fig 1(b), but the consistent behavior now occurs at -23 C instead of at -20 C The spread about the average is 0.026. Figure 1(d) is a combination of dependences seen in Figs 1(b) and 1(c) Two depths agree at each temperature and disagree at the other

temperature. Again, the spread at each temperature (about 0.015) is greater than our expected error.

The change in character of the temperature dependence seen in Fig. 1 supports the hypothesis that the structure of the some of the ice cores changed during our experiment. The close clustering of data in Fig. 1(b) for the vertical velocity from all depths at -20° suggests that core 336 maintained the same structure at both -10° and -20°, while the spread at -23° could be caused by a change in structure when the core was refrozen. In contrast, Fig. 1(c) suggests a different temperature dependence for the structure of core 350: the structure at -20°C is different than that at -10°C and -23°C. The close clustering of data at both -20°C and -23°C in Fig. 1(a) shows that the structure of core 276 did not change appreciably. The temperature dependence of other cores was too inconsistent to suggest a change in overall structure.

B. Depth dependence

We next turn to the depth dependence of the velocity. Table V illustrates the variability in the measured dependence of relative velocity on depth. The entries in Table V are the relative velocities averaged over depth for each core. Table V clearly illustrates the overall dependence on temperature in our data. The average over all cores and orientations has an increase in relative velocity of about 8% at -20°C and a smaller increase of 6% at -23°. The largest increase in relative velocity occurs for horizontal velocities at 45° to the c-axis, again suggesting that the ice cores are anisotropic. The largest increases occurred for the H/45° velocity of core 37; the average increase at -20 C is over 10% and the increase at -20°C at a depth of 94 cm was 12%, one of the largest we measured. The smallest increase (about 3%) occurred for the vertical velocity of core 336 at -23 C and a depth of 142 cm.

We found that the depth dependence was small (at most 5%) and was not consistent from core to core. Figure 2 gives four examples of the depth dependence. At each temperature, the velocity at the shallowest depth for each core was used as the

33

reference velocity. A reference velocity was used for each temperature to reduce the effects of the strong temperature dependence discussed above. The dashed line is a reference curve indicating zero depth dependence. The error bars indicate the expected uncertainty in the relative velocity (±0.009). Figure 2(a) is an example of core 276 that had little depth dependence at all three temperatures. Figure 2(b) illustrates a complicated depth dependence that changes with temperature and depth. Figure 2(c) shows that the relative horizontal velocity at 45° to the c-axis in core 37 has change of velocity with depth that depends on temperature. The relative velocity increases with depth at -10°C, changes very little at -20°C, and decreases at -23°C. Figure 2(d) shows that the relative horizontal velocity parallel to the c-axis in core 350 has a relatively constant gradient, but the gradient depends on temperature. The grouping of the -10° and -23° data away from the -20° data in Fig. 2(d) supports the hypothesis (discussed above) that the stucture of core 350 changed during our measurements.

The velocity gradients of the sea ice cores are given in Table VI. To calculate the velocity gradient, we assumed that the relative velocity was a linear function of depth for each core, and used linear least squares fit to the data to obtain the gradient. For the uncertainty in the gradient of the relative velocity, we took the inaccuracy of the relative velocity (0.9%) divided by the depth interval over which data were taken. The gradient and inaccuracy of the relative velocity were then multiplied by the reference velocity for each core to obtain the entries in Table VI

Three features are apparent from Table VI. First, while the change in relative velocity is small, the large value of velocity causes the gradients themselves to be quite large. The magnitude of the gradients are between about 20 and 400 s^{-1}. Second, both positive and negative gradients occur in sea ice cores. Third, the gradients of the smaller cores are larger, and have larger inaccuracies, than those of the smaller cores. The smaller horizontal cores (37, 276, and 336) have gradients from 89-392 s^{-1} and

34

uncertainties between 110-155 s^{-1} while the longer vertical cores (325 and 350) have gradients from 24-162 s^{-1} and a smaller uncertainty of about 50 s^{-1}. We feel that this difference indicates that the higher gradients of the smaller cores reflect changes in ice properties along the length of the core, and not a large scale trend. If this is true, the smaller gradients more accurately reflect the overall depth dependence of the velocity

Changes in the structure of the ice cores during the experiment could explain some of the changes in velocity with temperature. For example, we found a positive gradient for core 350 at -20°C and a negative gradient at both -10°C and -23 C. This change in sign is consistent with the possible change in structure for core 350 (discussed above) suggested by the grouping in temperature seen in Fig. 1(c). If this is true, the depth dependence would appear to be more sensitive to the structure of sea ice than the temperature dependence, which was fairly consistent for all five cores.

C. Anisotropy

The final feature we found in our data is a dependence of velocity on orientation, e., anisotropy. Figure 3 gives the measured ratios of horizontal to vertical velocity and the ratios of velocities in the horizontal plane for all temperatures, depths, and cores. A reference line for the velocity ratio of an isotropic material and the ±0.9% accuracy of the velocity ratios are also indicated. As seen in Fig. 3, the measured anisotropy is small, ±5%.

Figure 3(a) shows that the vertical velocity differs from the horizontal velocity in ce cores. The vertical velocity (V) is generally greater than the horizontal velocity at 0 to the c-axis (H-0) for core 276 and the horizontal velocity at 45 to the c-axis (H-45) for core 37 but is smaller than the horizontal velocity at 90 to the c-axis (H-90) for core 336. While H-0 V and H 90 appear to be relatively independent of V. H-45 V clearly tends toward the isotropic limit at larger V. Since we measured higher velocities primarily at lower temperatures, the dependence of anisotropy on V may actually be a dependence on temperature

35

Figure 3(b) gives the dependence of the measured velocity ratios in the horizontal plane on the horizontal velocity parallel to the c-axis, H-0°. At lower values of H-0° there is a clear difference between the ratio of H-45° to H-0° and the ratio of H-90° to H-0°; H-45° is about 2% larger than H-0° while H-90° is about 2% smaller. The difference is about the same for both cores suggesting that horizontal anisotropy is an intrinsic feature of sea ice. At higher values of H-0°, H-45° changes from being faster than H-0° to being slower. At higher values of H-0°, H-45° is also about the same as H-90°. As mentioned above, the dependence of the velocity ratios on H-0° may actually be a dependence on temperature.

Figures 4 and 5 investigate the dependence of the anisotropy on temperature. Figure 4 gives the ratio of vertical velocity to horizontal velocity (corresponding to Fig. 3 (a)), and Fig. 5 gives the ratios of velocities in the horizontal plane (corresponding to Fig. 3(b)). Reference lines indicating isotropy and error bars giving the uncertainty in the measured velocity ratios are also given. Figure 4 shows that the measured temperature dependences of H-0°/V, H-45°/V, and H-90°/V are different as might be expected from the temperature dependence of velocities discussed earlier. Figure 4(a) shows H-0°/V is almost independent of temperature in core 276 at all three depths. Figure 4(b) shows that H-45°/V in core 37 generally tends toward the isotropic limit with decreasing temperature. In core 336, H-90 is nearly equal to V at higher temperatures, but can be almost 6% larger and 3% smaller, depending on depth, at -23 C. This inconsistent behavior again points out the variability of ice properties from core to core.

Examination of Figs. 4(b), Fig 4(c), and Table V lends support to the hypothesis that the tendency for H-45 V toward the isotropic limit (Fig 3(a)) in core 37 at higher velocities is actually a dependence on temperature. Table V shows that the largest vertical velocities in core 37 were measured at -20 C and were about 7% higher than

36

values measured at -10°C. At -20°C, V decreased slightly from values at -23°C, but were still about 5% higher than V at -10°C. Figure 4(b) shows that H-45°/V is closest to 1.00 (except for the single point for 94 cm at -23°C) at -20°C, where highest velocities were measured. H-45°/V generally moves away from the isotropic limit at both higher and lower temperatures, where lower velocities were measured. The tendency toward the isotropic limit at higher velocities is thus consistent with a dependence on temperature.

Figure 5 shows that anisotropy in the horizontal plane has a fairly consistent dependence on temperature in the two cores we used. While the change in H-45°/H-0° with temperature is fairly small--only slightly larger than our measurement uncertainty at most depths--there does appear to be an increase, on average, between the ratio at -20° and that at -23°. Most of the curves from both cores have about the same shape, the same value at -10°C and -20°C, and an increase at -23°C, suggesting that there might be an intrinsic dependence of H-45°/H-0° on temperature. The offset of the individual curves from one another and the two curves that do not follow the general trend (74.5 cm for core 350 and 108 cm for core 325) suggests that the large spread in values of H-45°/H-0° in Fig. 3(b) is largely a result of the depth dependence of H-45°/H-0°. The average of H-45°/H-0° over all depths, given in Table VII, is consistent with these observations. The average is the same (0.979) for both -10°C and -20°C and increases only slightly to 0.989 at -23°C. The spread about the average is about the same as our measurement uncertainty.

In contrast with H-45°/H-0°, Fig. 5(b) shows that H-90°/H-0° has a clear dependence on temperature. H-90°/H-0° has its minimum value at -20°C and increases at both -23°C and -10 C. This same general shape occurs for all depths for both cores, suggesting that this is an intrinsic temperature dependence of H-90°/H-0°. Figure 5(b), combined with Table V, shows that the decrease in H-90°/H-0° with velocity seen in Fig. 3(b) is consistent with a dependence on temperature. The highest

37

values of H-0° were measured at -20°C, the same temperature where the lowest values of H-90°/H-0° were found.

Four examples of the depth dependence of the anisotropy are given in Fig. 6. The cores chosen are the same as those used for Fig. 4. H/0°/V in Fig. 6(a) is almost independent of depth. Considering our uncertainty in the velocity ratio, the nearly linear increase with depth in Fig. 6(a) is so gentle that the data are also consistent with no dependence on depth. Figure 6(b) shows that H-45°/H-0° for core 325 has the same mixed dependence on depth as H-45° in Fig. 2(b), again pointing out the possibility that core 325 has a complicated structure. Core 37 in Fig. 6(c) has a wide range of values for H-45°/V, from almost 1.00 to about 0.95 (some of the largest anisotropy in our data). There is almost no depth dependence at -10°C and -20°C. While Figs. 2(c) and 6(c) appear to have different depth dependences for core 37, they are similar in shape if the velocity ratios in Fig. 6(c) were normalized to their values at 94 cm. As in Fig. 2(d), Fig. 6(d) has a similar depth dependence at all three temperatures, with the -20°C data displaced from the -10°C and -23°C data. As mentioned above, this displacement may be due to a change in the structure of core 350 caused by loss of brine during the measurement at -10°C.

III. SUMMARY AND DISCUSSION

We measured the propagation velocity of ultrasonic compressional wave pulses at four orientations (vertical and at three horizontal directions) in five cores from first-year sea ice. Data were collected at three temperatures (-10°C, -20°C, and -23°C) and at several several depths into the ice sheet. Measured velocities were in the range of 3800-4500 m/s with an uncertainty of about 10%. More accurately measured relative velocities (±0.9%) were used to examine the temperature dependence, depth dependence, and anisotropy of compressional velocities in the sea ice cores. Consistent with reported[7] temperature gradients, the velocity at -20°C was higher (up

to 12%) than the velocity at -10°C. This temperature dependent increase occurred for all five cores, all three propagation directions, and at all depths where data were taken. The depth dependence was not consistent from core to core. The variability in depth dependence of velocity suggested that the structure of the sea ice cores is highly variable. Although the depth dependence was not consistently linear with depth, we made estimates of gradients of compressional velocity that fell between 20 and 400 s^{-1}. We found that the compressional wave velocity was anisotropic in all five of the sea ice cores. The anisotropy in our data was generally less than 5%. We found that vertical velocities were faster than horizontal velocities, that horizontal velocities perpendicular to the c-axis were slower than velocities parallel to the c-axis, and that horizontal velocities at 45° to the c-axis were either faster or slower than velocities parallel to the c-axis, depending primarily on temperature.

Our measurements of anisotropy of sea ice cores have some characteristics that differ from measurements made on fresh water ice. The anisotropy in these sea ice cores agrees in magnitude with data from fresh water ice crystals (velocity ratios of about 15%)[10] and from ice cores from the thick fresh water ice sheets in Antarctica and Greenland (velocity ratios 0f 1-2%).[11,12] However, our data show a qualitative difference in the direction of highest velocity. We found that the measured vertical velocity (perpendicular to the c-axis in the sea ice cores) is faster than horizontal velocity parallel to the c-axis. This differs from measurements on fresh water ice, in which the velocity along the c-axis is found to be faster than the velocity perpendicular to the c-axis,[10-12] but agrees with recent theoretical work[5] showing that the vertically oriented pore structure of sea ice can cause vertical velocities to exceed horizontal velocities. The different anisotropy of sea ice is also seen in the measured velocities at 45° to the c-axis, which were both faster and slower than velocities parallel to the c-axis.

Additional factors need to be taken into account to determine the in situ properties of sea ice. The effects of temperature gradients, pressure, salinity, and the properties of sea ice near the air and water interfaces were not examined in this experiment. Drainage of brine while coring and during our data collection at -10°C affected the volume of air inclusions in the ice cores, the salinity of refrozen ice, and the density of the core. Drainage may have also changed the size and connectivity of the vertically oriented pores, and hence the porosity of the ice cores. While we do not expect these changes to affect the qualitative aspects of our results, the magnitude of the temperature dependence and anisotropy may be different in situ than in the sea ice cores we used.

ACKNOWLEDGMENTS

APPENDIX

Compilation of vertical (V) and horizontal (H) velocities were measured for each core at three temperatures. Velocities are in units of m/s and temperatures in °C. Depth is the distance in cm from the top of the ice sheet. Horizontal velocities have three orientations relative to the c-axis of the ice crystals, 0° (H/0°), 45° (H/45°), and 90° (H/90°).

Core 276

	V			H/0°		
Depth	-10°C	-20°C	-23°C	-10°C	-20°C	-23°C
114	4146	4430	4393	4003	4287	4262
127	4135	4465	4352	4005	4343	4260
146	4108	4368	4376	4062	4306	4295

Core 37

	V			H/45°		
Depth	-10°C	-20°C	-23°C	-10°C	-20°C	-23°C
94	4096	4460	4333	3882	4364	4307
108	4167	4437	4351	3986	4338	4206
120	4151	4395	4358	3948	4325	4225

Core 336

	V			H/90°		
Depth	-10°C	-20°C	-23°C	-10°C	-20°C	-23°C
112	4157	4497	4355	4125	4488	4443
128	4122	4450	4393	4089	4435	4273
142	4116	4436	4231	4173	4541	4479

Core 325

Depth	H/0°			H/45°			H/90°		
	-10°C	-20°C	-23°C	-10°C	-20°C	-23°C	-10°C	-20°C	-23°C
74	4028	4424	4258	4009	4351	4247	4079	4325	4289
108	4042	4374	4351	3961	4437	4211	4074	4238	4253
125	3959	4392	4189	3895	4362	4256	4077	4360	4294
152	4069	4392	4203	3971	4258	4187	4098	4349	4361

Core 350

Depth	H/0°			H/45°			H/90°		
	-10°C	-20°C	-23°C	-10°C	-20°C	-23°C	-10°C	-20°C	-23°C
74.5	4121	4339	4365	3980	4235	4238	4162	4287	4386
119	4060	4410	4252	3918	4202	4202	4171	4397	4403
154	4003	4497	4267	3954	4330	4206	4022	4355	4268

REFERENCES

1. W. Weeks and A. Assur, "The Mechanical Properties of Sea Ice," U. S. Army Corps of Engineers Cold Regions Research and Engineering Laboratory monograph ıl-C3, U. S. Army Corps of Engineers Cold Regions Research and Engineering Laboratory, Hanover, New Hampshire (1967).

2. W. Weeks and S. Ackley, "The Growth, Structure and Properties of Sea Ice," U. S. Army Corps of Engineers Cold Regions Research and Engineering Laboratory monograph 82-1, U. S. Army Corps of Engineers Cold Regions Research and Engineering Laboratory, Hanover, New Hampshire (1982).

3. M. Biot, "Theory of Elastic Waves in a Fluid Saturated Porous Solid, Part I," J. Acoust. Soc. Am. **28**, 168-178 (1956).

4. M. Biot, "Theory of Elastic Waves in a Fluid Saturated Porous Solid, Part II" J. Acoust. Soc. Am. **28**, 179-191 (1956).

5. C. Yew and X. Weng, "A Study of Reflection and Refraction of Waves at the Interface of Water and Porous Sea Ice," to be published in The Journal of the Acoustical Society of America.

6. V. Bogorodskii, "The Elastic Characteristics of Ice." Sov. Phys.-Acoust. **4**, 19-23 (1958).

7. V. Bogorodskii, V. Gavrilo, A. Gusev, and V. Nikitin, "Measurements of the Speed of Ultrasonic Waves in Bering Sea Ice," Sov. Phys. Acoust. **21**, 286-287 (1975).

8. V. Bogorodskii, V. Gavrilo, and '. Nikitin, "Sound Propagation in Ice Crystallized from Salt Water." Sov. Phys.-Acoust., **22**, 158-159 (1976).

9. K. Hunkins, "Seismic Studies of Sea Ice." J. Geophy. Res. **65**, 3459-3472 (1960).

10. V. Bogorodskii and G. Khokhlov, "Acoustic Characteristics of Ice under Static Pressure," Sov. Phys.-Acoust., **13**, 14-17 (1967).

11. H. Hohnen and C. Bentley, "Ultrasonic Measurements on Ice Cores from Ross Ice Shelf, Antarctica, Drill Hole," Antarctic Journal of the United States **12**, 148-150 (1977).

12. A. Gow and H. Kohnen, "The Relationship of Ultrasonic Velocities to c-Axis Fabrics and Relaxation Characteristics of Ice Cores from Byrd Station, Antarctica," Journal of Glaciology **24**, 147-153 (1979).

13. D. Shirley and A. Anderson, "In Situ Measurement of Marine Sediment Acoustical Properties During Deep Coring," IEEE Trans. Geoscience Electronics **GE-13**, 163-169 (1975).

14. D. Shirley, D. Bell, and J. Hovem, "Laboratory and Field Studies of Sediment Acoustics," Applied Research Laboratories Technical Report No. 79-26 (ARL-TR-79-26), Applied Research Laboratories, The University of Texas at Austin (1979).

15. American Institute of Physics Handbook, 3rd edition, D. E. Gray coordinating editor (McGraw-Hill, New York, 1972).

TABLE I.   Density, compressional velocity, and rod velocity of calibration materials.

Material	Density (g/cc)	Compressional Velocity (m/s)	Rod Velocity (m/s)
Aluminum, rolled	2.7	6420	5000
Brass, yellow	8.6	4700	3480
Polystyrene	1.06	2350	1840

TABLE II.   Results of sensitivity analysis.

Parameter	Value	Expected Error	Percent Error in v	Percent Error in u
α	-2.1291×10^{-8} s/Hz	0.0143×10^{-8} s/Hz	2.73	0.21
β	1.5397×10^{-4} s	0.0080×10^{-4} s	2.80	0.16
T_i	10.6×10^{-6} s	1.43×10^{-6} s	5.01	0.26
L	10.000 cm	5.0×10^{-3} cm	0.05	0.10
f	5000 Hz	1 (Hz)	0.08	0.17
Total error			10.67	0.90

TABLE III. Ice core characteristics. Cores were cylindrical in shape and approximately 10.1 cm in diameter. The core number is the identification number in the CRREL storage system. Depth is distance into the ice from the air-ice interface.

core number	type	depth (cm)
350	vertical	74.5
		119.0
		154.0
325	vertical	74.0
		108.0
		125.0
		152.0
37	horizontal	94.0
		108.0
		120.0
276	horizontal	114.0
		127.0
		146.0
336	horizontal	112.0
		128.0
327	horizontal	142.0

Cores 336 and 327 are sections of the same core.

TABLE IV. Average vertical (V) and horizontal (H) velocities and
standard deviations at each temperature. Velocities
are in units of m/s and temperatures in °C. Horizontal
velocities have three orientations relative to the c-axis
of the ice crystals, 0° (H/0°), 45° (H/45°), and 90°
(H/90°).

Temperature	V	H/0°	H/45°	H/90°
-10°C	4133±24	4035±46	3950±41	4107±50
-20°C	4438±38	4376±61	4320±70	4378±91
-23°C	4349±49	4270±56	4229±35	4345±80

TABLE V. Depth average and standard deviations of relative vertical (V) and horizontal (H) velocities. Velocities are relative to the velocity at -10°C. Horizontal velocities have three orientations relative to the c-axis of the ice crystals, 0° (H/0°), 45° (H/45°), and 90° (H/90°).

Orientation	Core	-10°C	-20°C	-23°C
V	276	1.000	1.070±.008	1.059±.006
	37	1.000	1.071±.016	1.051±.007
	336	1.000	1.080±.002	1.047±.019
	Average	1.000	1.074±.010	1.052±.012
H/0°	276	1.000	1.072±.012	1.062±.004
	325	1.000	1.092±.014	1.056±.016
	350	1.000	1.088±0.35	1.058±0.10
	Average	1.000	1.085±.021	1.058±0.12
H/45°	37	1.000	1.103±.019	1.078±.019
	325	1.000	1.099±.024	1.067±.017
	350	1.000	1.077±.016	1.067±.005
	Average	1.000	1.094±.022	1.071±.018
H/90°	336	1.000	1.087±.002	1.065±.018
	325	1.000	1.058±.012	1.053±.008
	350	1.000	1.056±.026	1.057±.004
	Average	1.000	1.066±.021	1.058±.011
Overall average		1.000	1.080±.021	1.060±.015

TABLE VI.   Velocity gradients and uncertainties for three temperatures and three orientations relative to the c-axis of the ice crystals, 0° (H/0°), 45° (H/45°), and 90° (H/90°). Gradient is in units of s^{-1}.

Orientation	Core	-10°C	-20°C	-23°C
V	37	229±143	-254±156	100±152
	276	-116±116	-217±124	-44±123
	336	-141±125	-211±124	-392±131
H/0°	276	196±112	34±120	111±119
	325	24±48	-35±53	-106±51
	350	-148±45	195±48	-127±48
H/45°	37	268±136	-153±153	-327±151
	325	-72±48	-122±52	-59±51
	350	-40±44	110±47	-34±47
H/90°	325	24±49	61±52	94±51
	336	157±124	166±135	89±133
	350	-162±46	94±47	-140±48

50

TABLE VII. Average ratio of horizontal velocities and spread about the average. The average is over all depths for cores 325 and 350. Horizontal velocities have three orientations relative to the c-axis of the ice crystals, 0° (H/0°), 45° (H/45°), and 90° (H/90°).

Ratio	-10°C	-20°C	-23°C
H-45°/H-0°	0.979±0.011	0.979±0.020	0.989±0.017
H-90°/H-0°	1.014±0.010	0.983±0.012	1.013±0.022

FIGURE CAPTIONS

Figure

1   Dependence of relative velocity on temperature with depth below the ice surface as a parameter: (a) vertical velocity (V) for core 276; (b) V for core 336; (c) horizontal velocity at 90° to the c-axis (H-90°) for core 350; and (d) horizontal velocity parallel to the c-axis (H-0°) for core 325. The error bars give the uncertainty in the measured velocity ratio.

2   Dependence of relative velocity on depth with temperature as a parameter: (a) horizontal velocity at 0° to the c-axis (H-0°) for core 276; (b) horizontal velocity at 45° to the c-axis (H-45°) for core 325; (c) H-45° for core 37; and (d) horizontal velocity parallel to the c-axis (H-0°) for core 350. The horizontal line at a relative velocity of 1.00 is a reference line indicating no depth dependence. The error bars give the uncertainty in the measured velocity ratio.

3   Measured velocity anisotropy: (a) ratio of vertical velocity (V) to horizontal velocity at 0° (H-0°), 45° (H-45°), and 90° (H-90°) to the c-axis; and (b) ratio of H-45° and H-90° to H-0°. The horizontal line at a relative velocity of 1.00 is a reference line indicating no depth dependence. The error bars give the uncertainty in the measured velocity ratio.

4   Dependence of measured velocity anisotropy on temperature with depth as a parameter: (a) the ratio of vertical velocity to horizontal velocity at 0° to the c-axis for core 276; (b) the ratio of vertical velocity (V) to horizontal velocity at 45° to the c-axis for core 37; and (c) the ratio of vertical velocity to horizontal velocity at 90° to the c-axis for core 336. The horizontal line at a relative velocity of 1.00 is a reference line indicating no depth dependence. The error bars give the uncertainty in the measured velocity ratio.

5   Dependence of measured velocity anisotropy in the horizontal plane on temperature with depth as a parameter: (a) the ratio of velocity at 45° to the c-axis to the velocity parallel to the c-axis for cores 325 and 350; (b) the ratio of velocity perpendicular to the c-axis to the velocity parallel

52

to the c-axis for cores 325 and 350. The horizontal line at a relative velocity of 1.00 is a reference line indicating no depth dependence. The error bars give the uncertainty in the measured velocity ratio.

6   Velocity ratio as a function of depth with temperature as a parameter: (a) the ratio of vertical velocity (V) to the horizontal velocity parallel to the c-axis (H-0°) for core 276; (b) the ratio of V to the horizontal velocity perpendicular to the c-axis (H-90°) for core 325; (c) the ratio of horizontal velocity at 45° to the c-axis (H-45°) to H-0° for core 37; and (d) the ratio of H-90° to H-0° for core 350. The horizontal line at a velocity ratio of 1.00 is the reference line indicating no dependence on propagation direction. The error bars give the uncertainty in the measured velocity ratio.
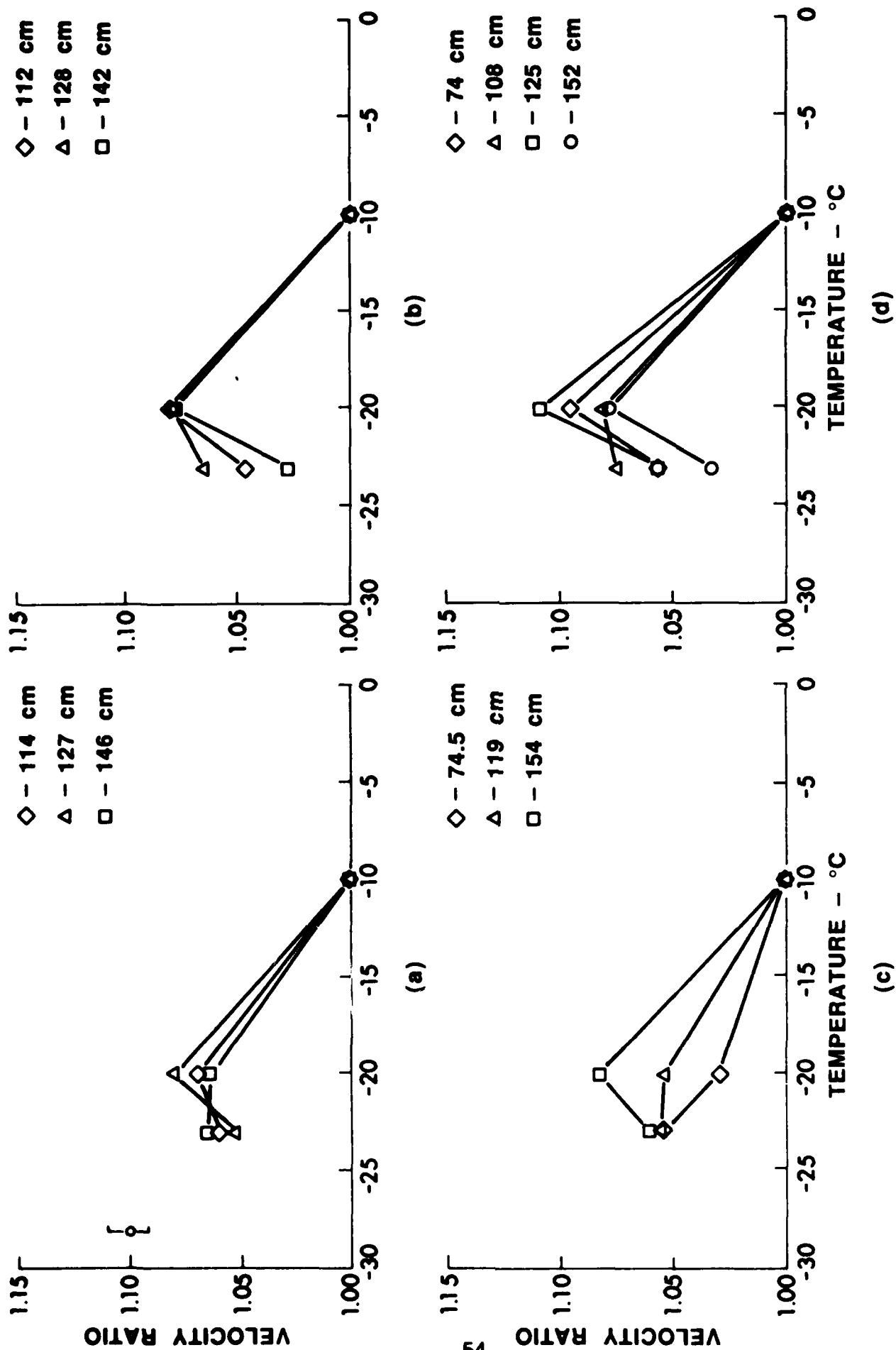
Figure 1
Vidmar
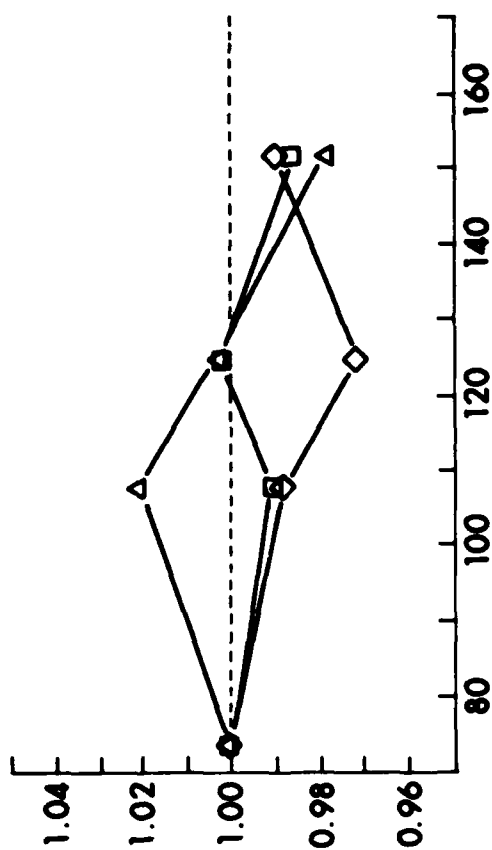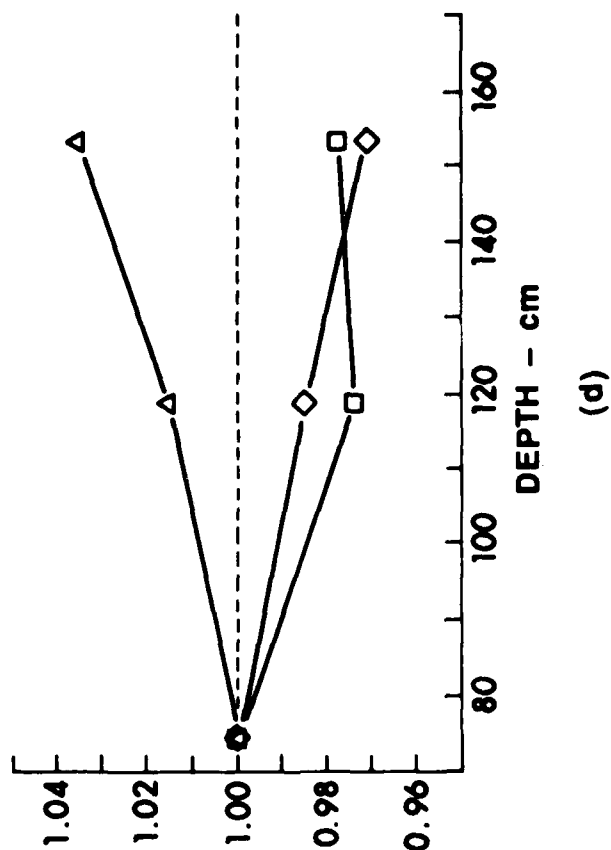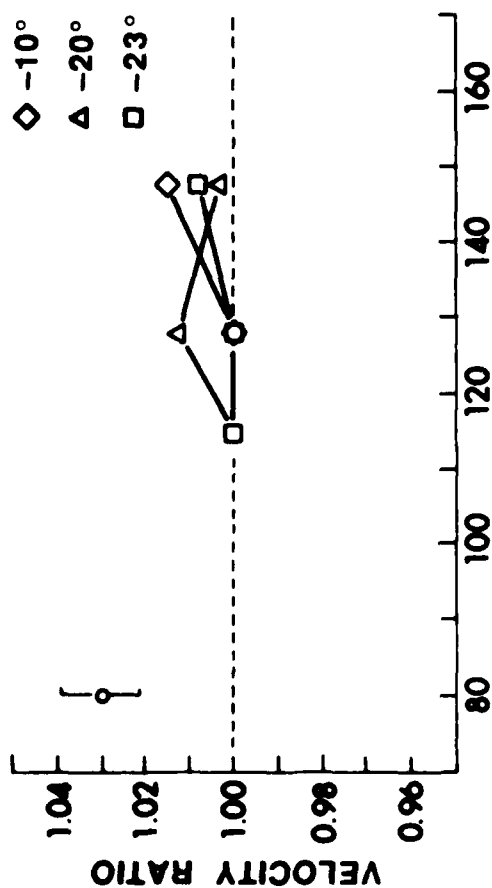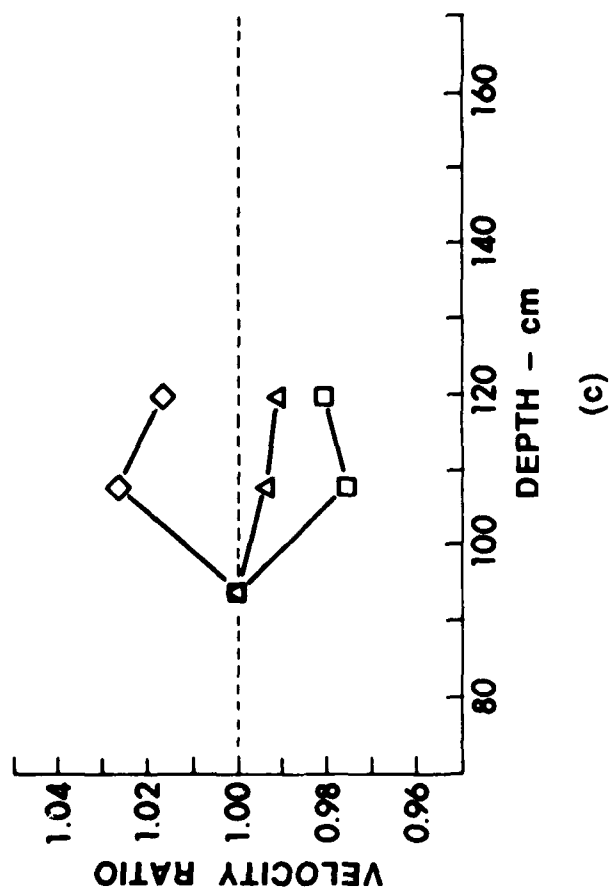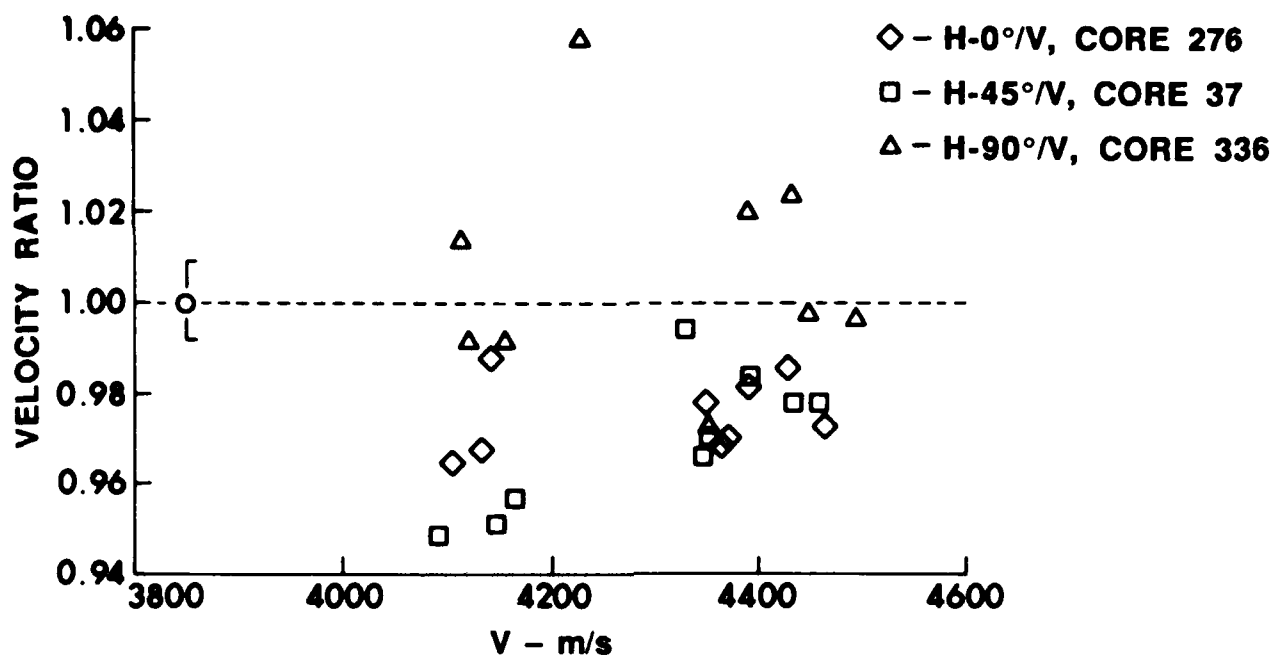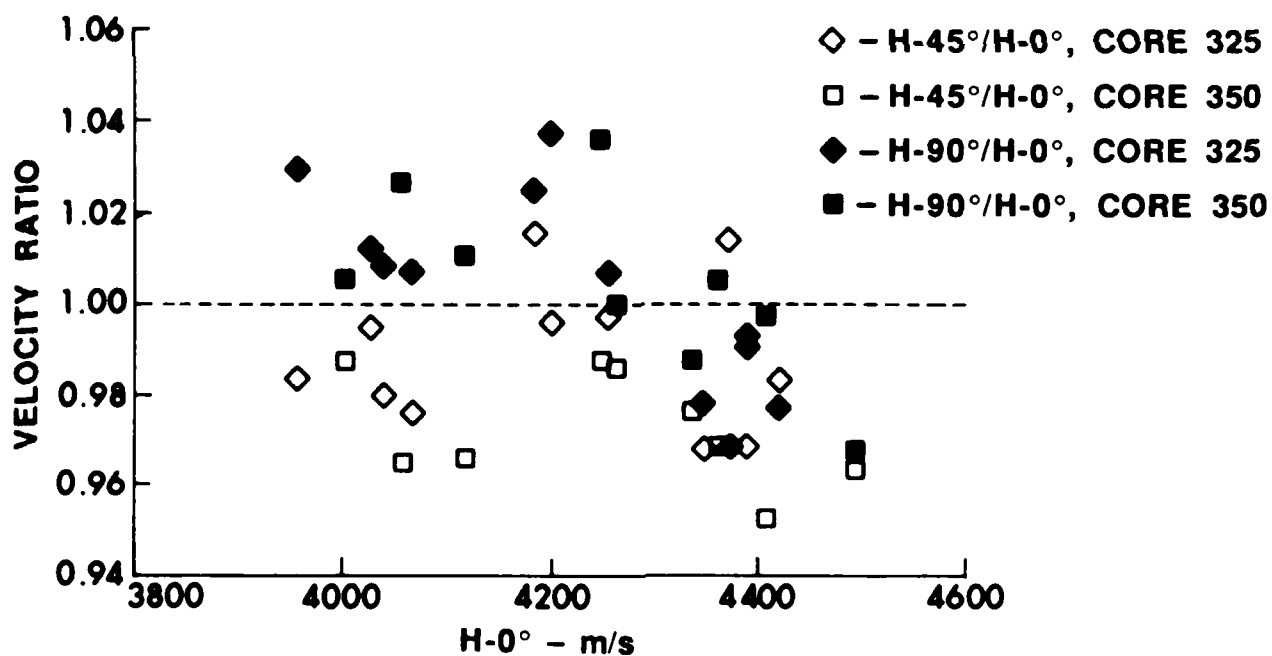
Figure 2
Vidmar

(a)

(b)

(a)

(b)

TEMPERATURE – °C

(c)

(a)

(b)
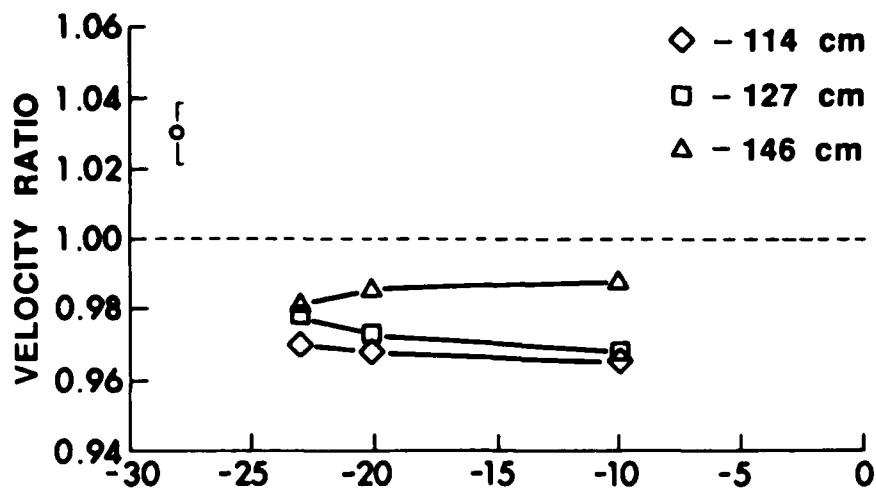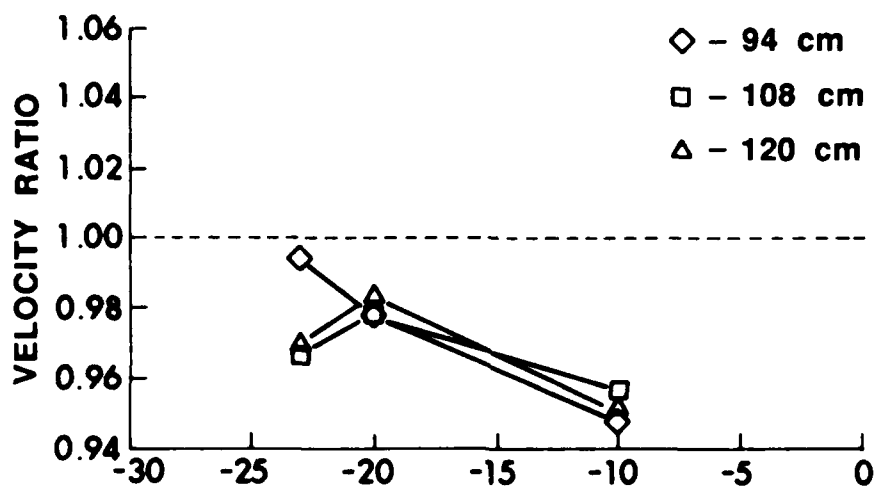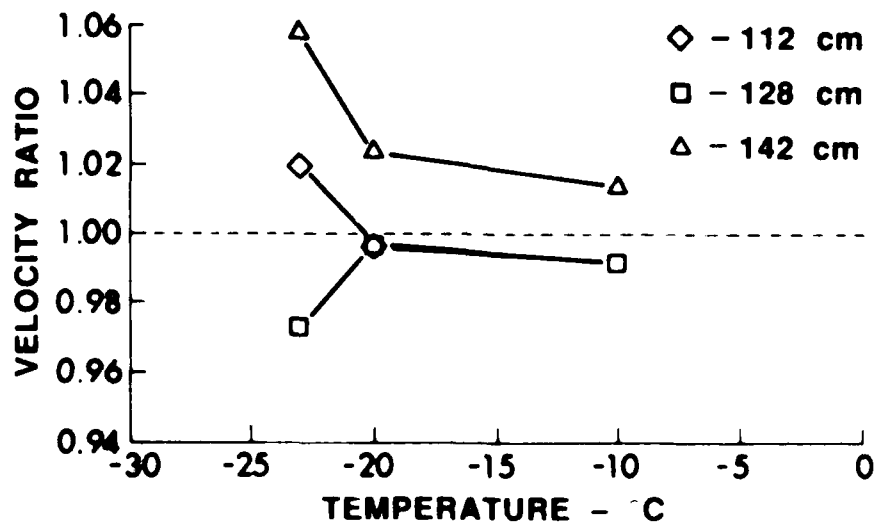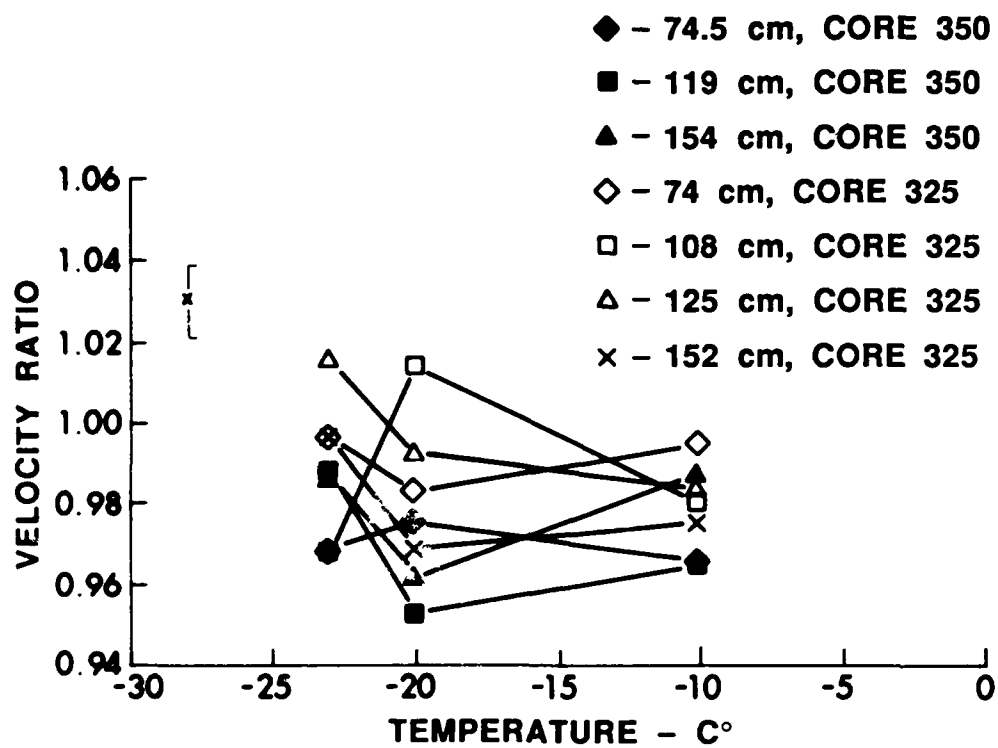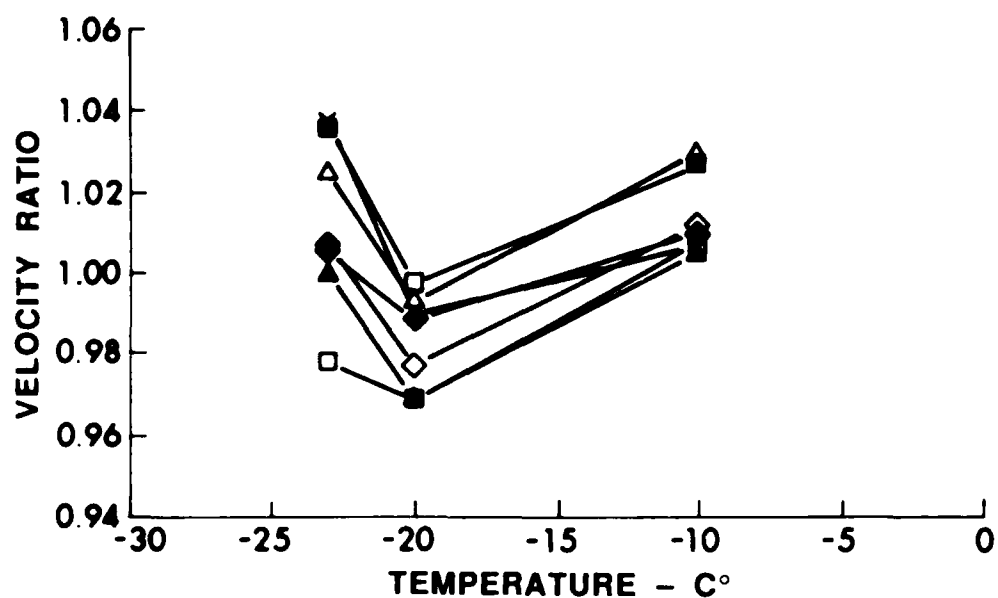
Figure 6
Vidmar

APPENDIX B

Documentation Produced under Contract N00014-84-C-0195

1. C. H. Yew, "Use of Penetrators to Estimate the Properties of Ice in the Arctic Region," presented at Arctic Oceanography Conference and Workshop held at NSTL, MS, 11-14 June 1985.
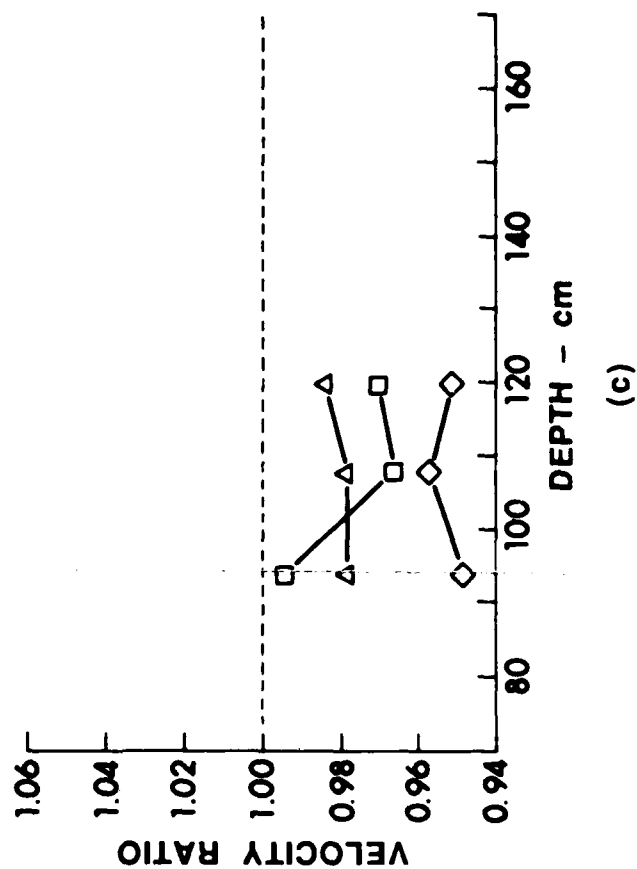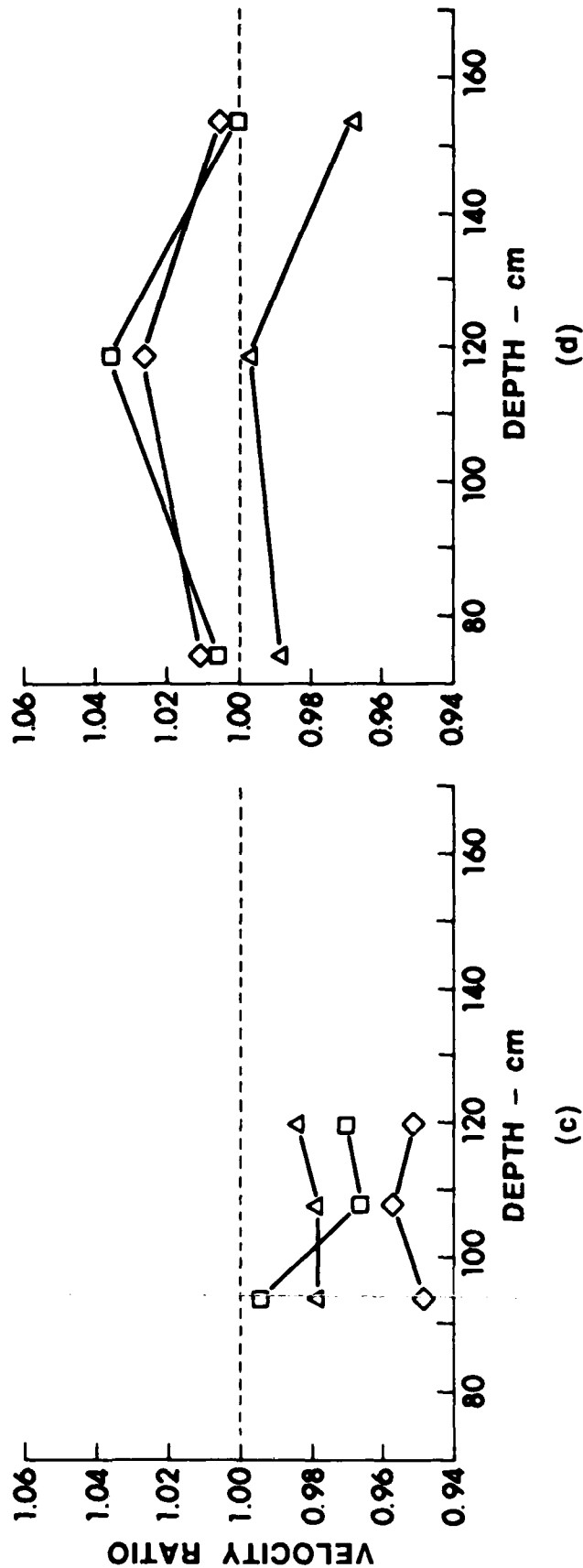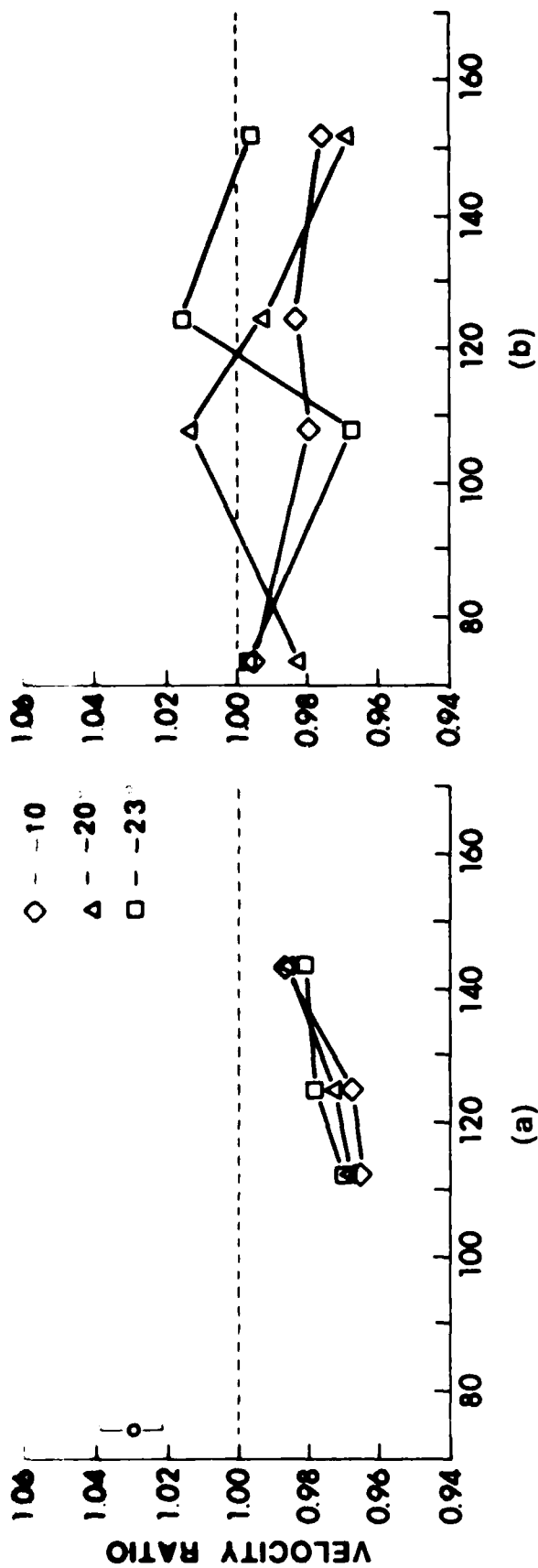
2. C. H. Yew, "Use of Penetrators To Estimate the Properties of Ice in the Arctic Region," in the Proceedings of the Arctic Oceanography Conference and Workshop, 11-14 June 1985, Naval Ocean Research and Development Activity, NSTL, Mississippi (1985).

3. P. J. Vidmar and J. B. Lindberg, "Anisotropy of Compressional Velocity in Sea Ice Cores," to be presented at the 113th Meeting of the Acoustical Society of America to be held at Indianapolis, Indiana, May 11-15 1987.

4. P. J. Vidmar and J. B. Lindberg, "Compressional Velocity of Seas Ice Cores," Applied Research Laboratories Technical Paper No. 87-3 (ARL-TP-87-3), Applied Research Laboratories, The University of Texas at Austin, Austin, Texas (January 1987). Submitted for publication in The Journal of the Acoustical Society of America.

REFERENCES

1. W. F. Weeks and A. Assur, "The Mechanical Properties of Sea Ice," U. S. Army Corps of Engineers Cold Regions Research and Engineering Laboratory monograph II-C3, U. S. Army Corps of Engineers Cold Regions Research and Engineering Laboratory, Hanover, New Hampshire, 1967.

2. W. Weeks and S. F. Ackley, "The Growth, Structure and Properties of Sea Ice", CARREL Monograph 82-1, U. S. Army Corps of Engineers Cold Regions Research and Engineering Laboratory, Hanover, New Hampshire, 1982.

3. M. A. Biot, "Theory of Elastic Waves in a Fluid Saturated Porous Solid, Part I," J. Acoust. Soc. Am. **28**, 168-178 (1956).

4. M. A. Biot, "Theory of Elastic Waves in a Fluid Saturated Porous Solid, Part II" J. Acoust. Soc. Am. **28**, 179-191 (1956).

5. C. H. Yew and X. Weng, "A Study of Reflection and Refraction of Waves at the Interface of Water and Porous Sea Ice," accepted for publication in The Journal of the Acoustical Society of America.

6. P. J. Vidmar and J. B. Lindberg, "Compressional Velocity of Sea Ice Cores," Applied Research Laboratories Technical Paper No. 87-3 (ARL-TP-87-3), Applied Research Laboratories, The University of Texas at Austin, Austin, Texas (January 1987). Submitted for publication in The Journal of the Acosutical Society of America.

7. V. V Bogorodskii and G. P. Khokhlov, "Acoustic Characteristics of Ice under Static Pressure," Sov. Phys.-Acoust. **13**, 14-17 (1967).

8. H. Hohnen and C. R. Bentley, "Ultrasonic Measurements on Ice Cores from Ross Ice Shelf, Antarctica, Drill Hole," Antarctic Journal of the United States **12**, 148-150 (1977).

9. A. J. Gow and H. Kohnen, "The Relationship of Ultrasonic Velocities to c-Axis Fabrics and Relaxation Characteristics of Ice Cores from Byrd Station, Antarctica," Journal of Glaciology 24, 147-153 (1979).

10. C. H. Yew, "Use of Penetrators To Estimate the Properties of Ice in the Arctic Region," in Proceedings of the Arctic Oceanography Conference and Workshop, 11-14 June 1985, Naval Ocean Research and Development Activity, NSTL, Mississippi.

11. D. J. Shirley and A. L. Anderson, "In Situ Measurement of Marine Sediment Acoustical Properties During Deep Coring", IEEE Trans. on Geoscience Electronics GE-13, 163-169 (1975).

12. D. J. Shirley, D. W. Bell, and J. M. Hovem, "Laboratory and Field Studies of Sediment Acoustics," Applied Research Laboratories Technical Report No. 79-26 (ARL-TR-79-26), Applied Research Laboratories, The University of Texas at Austin, Austin, Texas, 12 June 1979.

13. V. V. Bogorodskii, "The Elastic Characteristics of Ice," Sov. Phys.-Acoust. 4, 19-23 (1958).

14. V. V. Bogorodskii, V. P. Gavrilo, A. V. Gusev, and V. A. Nikitin, "Measurements of the Speed of Ultrasonic Waves in Bering Sea Ice," Sov. Phys.-Acoust. 21, 286-287 (1975).

15. V. V. Bogorodskii, V. P. Gavrilo, and V. A. Nikitin, "Sound Propagation in Ice Crystallized from Salt Water," Sov. Phys.-Acoust. 22, 158-159 (1976).

16. K. Hunkins, "Seismic Studies of Sea Ice," J. Geophys. Res. 65, 3459-3472 (1960).

17. Y. Sato, "Analysis of Dispersed Surface Waves by Measure of Fourier Transform I," Bull. Earthq. Res. Inst. 33, 33-50 (1955).

18.   Y. Sato, "Analysis of Dispersed Surface Waves by Measure of Fourier Transform II," Bull. Earthq. Res. Inst. **34**, 9-18 (1955).

19.   Y. Sato, "Analysis of Dispersed Surface Waves by Measure of Fourier Transform III," Bull. Earthq. Res. Inst. **34**, 131-138 (1955).

20.   C. H. Yew and C. S. Chen, "Study of Linear Wave Motions Using FFT and Its Potential Application to Non-Destructive Testing," Int. J. Engn. Sci. **18**, 1027-1036 (1980).

21.   J. A. Ware and K. Aki, "Continuous and Discrete Inverse Scattering Problem in a Stratified Elastic Medium, I. Plane Waves at Normal Incidence," J. Acoust. Soc. Am. **45**, 911-921 (1965).

DISTRIBUTION LIST FOR
ARL-TR-87-6
UNDER CONTRACT N00014-84-C-0195

Copy No.

Chief of Naval Research
Office of Naval Research
Department of the Navy
Arlington, VA 22217-5000

Copy No.	
1	Attn: Library
2	R. F. Obrochta (Code 1125AR)
3	G. L. Johnson (code 1125)
4	R. Fitzgerald (Code 1125OA)
5	J. Heacock (Code 1125GG)
6	J. H. Kravitz (Code 1125GG)

Commanding Officer
Naval Ocean Research and Development Activity
NSTL Station, MS 39529-5000

7	Attn: Library
8	B. Adams (Code 110A)
9	J. Matthews (Code 222)
10	D. Del Balzo (Code 244)
11	R. Wagstaff (Code 425)
12	H. Ali (Code 425)
13	J. Caruthers (Code 220)
14	D. King (Code 321)
15	D. Ramsdale (Code 242)
16	W. Moseley (Code 200)
17	T. Goldsberry (Code 240)

Office of Naval Research Field Detachment
Bay St. Louis
NSTL, MS 39529-5000

18	Attn: E. D. Chaika (Code 132)
19	B. N. Wheatly (Code 132)

Distribution list for ARL-TR-87-6 under Contract N00014-84-C-0195 (cont'd)

Copy No.

	Director Naval Research Laboratory Washington, D.C. 20375
20	Attn: Library
21	O. Diachok (Code 5128)
22	C. Votaw (Code 5123)
23	R. Dicus (Code 5128)
24	D. Bradley (Code 5100)
25	F. Ingenito (Code 5160)
26	W. Kuperman (Code 220)
27	M. F. Czarnecki (Code 5110)
28	R. N. Baer (Code 5160)
29	R. Pitre (Code 5160)
30	R. Gragg (Code 5160)

	Chief of Naval Research Office of Naval Technology Arlington, VA 22217-5000
31	Attn: J. T. Warfield (Code 234)

	Commanding Officer Naval Ocean Systems Center San Diego, CA 92152-5000
32	Attn: Library
33	H. Bucker (Code 541)
34	D. Gordon (Code 711)

	Commander Naval Surface Weapons Center White Oak Laboratory Silver Spring, MD 20910
35	Attn: Library

Copy No.

Commander
David W. Taylor Naval Ship Research and
 Development Center
Bethesda, MD 20034
36   Attn: Library

Commanding Officer
Naval Oceanographic Office
Bay St. Louis
NSTL, MS 39522-5001
37   Attn: Library
38   W. Jobst (Code 7300)
39   R. Hecht (Code 7310)

Commander
Naval Air Development Center
Warminster, PA 18974
40   Attn: Library
41   C. L. Bartberger

Officer in Charge
New London Laboratory
Naval Underwater Systems Center
New London, CT 06320
42   Attn: Library
43   P. Herstein (Code 33A3)
44   R. Deavenport (Code 3332)
45   W. Carey (Code 33A)
46   D. Lee (Code 3342)

Distribution list for ARL-TR-87-6 under Contract N00014-84-C-0195
(cont'd)

Superintendent
Naval Postgraduate School
Monterey, CA 93943
47   Attn: Library
48   H. Medwin

Commander
Naval Coastal Systems Center
Panama City, FL 32407
49   Attn: Library

50   Commander
Naval Intelligence Support Center
Washington, D.C. 20390

51 - 62   Commanding Officer and Director
Defense Technical Information Center
Cameron Station, Building 5
5010 Duke Street
Alexandria, VA 22314

Woods Hole Oceanographic Institution
86-95 Water Street
Woods Hole, MA 02543
63   Attn: Library
64   R. Spindel
65   J. Lynch
66   G. Frisk

Distribution list for ARL-TR-87-6 under Contract N00014-84-C-0195 (cont'd)

Copy No.

Science Applications, Inc.
1710 Goodridge Drive
McLean, VA 22101
67   Attn: C. Spofford
68   R. Keenan
69   L. Dozier

Applied Research Laboratory
The Pennsylvania State University
P.O. Box 30
State College, PA 16801
70   Attn: Library
71   S. McDaniel
72   D. McCammon

Applied Physics Laboratory
The University of Washington
1013 N. E. 40 St.
Seattle, WA 98105
73   Attn: Library
74   R. Francois

Marine Physical Laboratory of the
  Scripps Institution of Oceanography
The University of California, San Diego
San Diego, CA 92132
75   Attn: Library
76   F. Fisher

Polar Research Laboratory, Inc.
123 Santa Barbara Street
Santa Barbara, CA 93101
77   Attn: B. Buck

Distribution list for ARL-TR-87-6 under Contract N00014-84-C-0195
(cont'd)

<u>Copy No</u>.

Bell Telephone Laboratories, Inc.
Whippany Road
Whippany, NJ 07961
78   Attn: Library
79   A. Carter
80   R. Patton

Planning Systems, Incorporated
7900 Westpark Drive
McLean, VA 22101
81   Attn: R. Cavanaugh
82   B. Brunson

Planning Systems, Incorporated
115 Christian lane
Slidell, LA 70458
83   Attn: J. Paquin
84   M. R. Bradley

School of Mechanical Engineering
Georgia Institute of Technology
Atlanta, GA 30332
85   Attn: A. D. Pierce
86   P. Rogers

Department of Geology and Geophysics
Geophysical and Polar Research Center
Lewis G. Weeks Hall for Geological Sciences
The University of Wisconsin, Madison
1215 W. Dayton Street
Madison, WI 53706
87   Attn: C. S. Clay

Distribution list for ARL-TR-87-6 under Contract N00014-84-C-0195
(cont'd)

<u>Copy No</u>.

       Bolt, Beranek, & Newman, Inc.
       50 Moulton Street
       Cambridge, MA 02138
88   Attn: Library
89   H. Cox

       Bolt, Beranek, & Newman, Inc.
       1300 North 17th Street
       Arlington, VA 22209
90   Attn: R. Henrick

       Director
       North Atlantic Treaty Organization
       SACLANT ASW Research Centre
       APO New York 09019
91   Attn: Library
92   F. Jensen
93   T. Akal
94   T. Muir

       Defence Research Establishment Pacific
       FMO Victoria, BC
       VOS 1B0
       CANADA
95   Attn: Library
96   N. R. Chapman

Distribution list for ARL-TR-87-6 under Contract N00014-84-C-0195 (cont'd)

<u>Copy No</u>.

Defence Research Establishment Atlantic
9 Grove Street
P.O. Box 1012
Dartmouth, NS
CANADA
97   Attn: Library
98   D. Chapman

Rosenteil School of Marine and
  Atmospheric Science
The University of Miami
10 Rickenbacker Causeway
Miami, FL 33149
99   Attn: H. DeFarrari

Applied Physics Laboratory
The John Hopkins University
John Hopkins Road
Laurel, MD 20810
100   Attn: Library
101   A. Boyles

Department of Ocean Engineering
Massachusetts Institute of Technology
Cambridge, MA 02139
102   Attn: I. Dyer
103   G. Duckworth
104   A. Baggeroer

The University of Miami
10 Rickenbacker Causeway
Miami, FL 33149
105   Attn: F. Tappert

77

Copy No.

Defence Scientific Establishment
HMNZ Dockyard
Devonport, Auckland
NEW ZEALAND
116   Attn: Library
117   K. M. Guthrie
118   R. Bannister

The Lamont-Doherty Geological Observatory
Columbia University
Palisades, NY 10964
119   Attn: Library
120   R. D. Stoll
121   H. Kutschale

Department of Oceanography
Texas A&M University
College Station, TX 77843
122   Attn: A. L. Anderson

123   Environmental Sciences Group, ARL:UT

124   Nancy R. Bedford, ARL:UT

125   Karl C. Focke, ARL:UT

126   David E. Grant, ARL:UT

127   Thomas Griffy, ARL:UT

128   John M. Huckabay, ARL:UT

129   Robert A. Koch, ARL:UT

Distribution list for ARL-TR-87-6 under Contract N00014-84-C-0195
(cont'd)

Copy No.

130   Stephen K. Mitchell, ARL:UT

131   David W. Oakley, ARL:UT

132   Susan G. Payne, ARL:UT

133   Clark S. Penrod, ARL:UT

134   Carol V. Sheppard, ARL:UT

135   Jack A. Shooter, ARL:UT

136   Arnold J. Tucker, ARL:UT

137   Bernard F. Tupa, ARL:UT

138   Paul J. Vidmar, ARL:UT

139   Evan K. Westwood, ARL:UT

140   Joseph L. Willman, ARL:UT

141   Library, ARL:UT

142 - 149   Reserve, ARL:UT

END

5-81

DTIC